Received: 22 July 2021 | Revised: 18 October 2022 | Accepted: 23 May 2023

DOI: 10.1002/rnc.6818

RESEARCH ARTICLE

WILEY

Passivity-based control design frameworks for hybrid nonlinear time-varying dynamical systems

Esmaeil Sharifi | **Christopher J. Damaren**

Institute for Aerospace Studies, University of Toronto, Toronto, Ontario, Canada

Correspondence
Esmaeil Sharifi, Institute for Aerospace Studies, University of Toronto, Toronto, Ontario, Canada M3H 5T6.
Email: esmaeil.sharifi@mail.utoronto.ca

Abstract

This article proposes two novel passivity-based control design frameworks for hybrid nonlinear dynamical systems involving an interacting mixture of continuous-time and discrete-time dynamics whose dynamical properties evolve periodically over time. By deriving the Kalman–Yakubovich–Popov (KYP) conditions characterizing dissipativeness for hybrid nonlinear time-dependent dynamical systems, a hybrid computational algorithm, which alternates between continuous-time and discrete-time subsystems at an appropriate sequence of time instants, is then proposed to solve the resultant equations in an interacting manner. Two passivity-based control schemes are then developed by utilizing the foregoing KYP conditions in tandem with the passivity theorem. The overall framework consists mainly of three steps. The hybrid output dynamics of the plant are first determined judiciously to satisfy the passivity specifications. A hybrid nonlinear controller is then designed to meet the input strict passivity requirements. The stability of the closed-loop system is finally established by interconnecting the plant and the controller through negative feedback. Practical considerations for appropriately implementing the derived hybrid algorithms are then discussed in detail. The efficacy of the proposed control schemes is ultimately assessed via a multi-dimensional system with a hybrid source of actuation.

KEYWORDS

dissipative dynamical systems, Galerkin/collocation-based approximation, hybrid dynamical systems, hybrid nonlinear time-varying control, Kalman–Yakubovich–Popov conditions, passivity-based control design

1 | INTRODUCTION

Hybrid dynamical systems, as an emerging discipline within dynamical systems theory and control, comprise an interacting collection of dynamical systems involving a mixture of continuous-time and discrete-time dynamics. Exhibiting heterogeneous dynamics, the evolution of which occurs both continuously (flow) and discontinuously (jump) on appropriate manifolds, hybrid dynamical systems consist mainly of three elements: a continuous-time set of differential equations, which characterizes the motion of the dynamical system between discrete-time events; a discrete-time set of difference equations, which governs discontinuous changes in the system state; and a criterion to determine when discrete-time dynamics are to be applied.[1]

Hybrid dynamical systems can be categorized into four distinct groups. Some systems are intrinsically hybrid in nature; bouncing balls and mechanical systems subject to unilateral constraints are examples of such systems.[2] In the next group, continuous-time dynamics are collaboratively augmented by discrete-time dynamics in order to, amongst other objectives, improve the performance of the system. Modern spacecraft attitude control systems epitomize systems of this nature where magnetic torquers are used in tandem with mechanical actuators (like reaction wheels and thrusters) to resolve instantaneous underactuation pertinent inherently to the magnetic-based actuation, thereby improving the system performance.[3] Hybrid paradigms can also occur in a wide range of applications when a multi-modal control architecture is employed to regulate the behavior of a complex engineering system.[4,5] A special class of this group emerges when control frameworks involving logic, timers, clocks, and other digital devices are applied to continuous-time dynamics; sample-and-hold control systems and control systems that involve hysteresis exemplify such systems.[6] Also included in this group are systems whose control algorithms encompass multiple continuous-time schemes which switch from one to another, once a specific criterion is met, to achieve certain prescribed objectives.[7,8] The next category, which introduces a more complicated class of the preceding group, represents systems with hybrid paradigms in both dynamics (plant) and control where dynamics with heterogeneous structures are regulated by hybrid controllers involving an interacting pair of continuous-time and discrete-time control inputs which additionally, once a criterion is met, switch to logical decision-making control laws.

Motivated by applications of systems with heterogeneous dynamics whose dynamical properties evolve over time while simultaneously interacting with their surrounding environments, this article proposes two novel passivity-based control design architectures for hybrid nonlinear time-dependent dynamical systems. Establishing a quantitative relationship between the energy injected into and dissipated by a system, the notion of passivity provides a fundamental framework for the analysis and control design of dynamical systems via exerting a constraint on the amount of energy they exchange through their input–output ports. The origin of this concept can be traced back to development in the linear passive network theory in the 1950s[9] and, specifically, the stability analysis of feedback systems through positive real matrices in the 1960s.[10–13] Nevertheless, the first general input–output energy-based system description was proposed by Willems via introducing the dissipativity theory for linear dynamical systems.[14,15] This pioneering work was then followed by characterizing dissipativeness in the input–output sense for a large class of nonlinear systems.[16–18] Using the notion of dissipativity, Reference 18 subsequently presented general stability criteria for the feedback interconnection of autonomous nonlinear dynamical systems. Providing a generalized interpretation of energy balance in terms of the stored energy and the dissipated energy over heterogeneous dynamics, the dissipativity theory was then generalized to hybrid nonlinear dynamical systems with an interacting mixture of continuous-time and discrete-time dynamics.[19] Building on these results, stability criteria characterizing Lyapunov, asymptotic, and exponential properties for the feedback interconnection of hybrid nonlinear dissipative dynamical systems were derived in Reference20. The notion of dissipativity has also been extended to a different variety of dynamical systems, including discrete-time nonlinear systems for observer design purposes,[21–23] nonnegative and compartmental systems,[24,25] large-scale systems,[26,27] port-controlled Hamiltonian systems,[28,29] and stochastic systems[30,31] to name but a few.

Although the control theory for hybrid nonlinear dissipative dynamical systems involving an interacting amalgam of continuous-time and discrete-time dynamics is well-developed (see Haddad et al.[1] and references therein), it has found no practical applications due primarily to a lack of efficient numerical schemes for dealing effectively with such systems. This article aims to bridge the gap between theory and practice by developing two passivity-based control design frameworks for hybrid nonlinear dynamical systems whose dynamical properties evolve periodically over time. In this regard, the Kalman–Yakubovich–Popov (KYP) conditions proposed in Reference19, which characterize dissipativity for hybrid nonlinear time-invariant dynamical systems, are first extended to systems with time-variations. A hybrid computational architecture, which alternates between continuous-time and discrete-time subsystems at an appropriate sequence of time instants, is then proposed to solve the resultant equations in an interacting manner. Utilizing the derived time-varying KYP (TV-KYP) conditions and the passivity theorem collaboratively, two passivity-based control schemes are ultimately developed for nonlinear time-dependent dynamical systems with heterogeneous dynamics.

By employing the control schemes proposed in this research work, not only are interactions between continuous-time and discrete-time dynamics allowed in accordance with the resetting criterion, but feedback controllers are also synthesized by considering the full nonlinear dynamics of the system. As a consequence, in contrast to the traditional approach in which the hybrid nature of systems is suppressed by converting them into either purely discrete-time or purely continuous-time entities, the heterogeneous structure of the dynamical system to be controlled is effectively exploited over the entire operating range of the system through a hybrid pair of control inputs which alternates between continuous-time and discrete-time subsystems at an appropriate sequence of time instants. Moreover, since the stability of the closed-loop

system is guaranteed in accordance with energy-based system properties, the proposed control schemes are expected to exhibit enhanced robustness with respect to uncertainties and measurement noise effects.[3,32]

The remainder of this article is organized as follows. The preliminary definitions and main theorems associated with dissipative dynamical systems are presented in Section 2. Two novel passivity-based control design frameworks are then proposed for hybrid nonlinear time-dependent dynamical systems in Section 3. Section 4 describes practical considerations for appropriately implementing the proposed hybrid algorithms. The functionally of the proposed hybrid controllers is lastly evaluated via a multi-state hybrid system in Section 5.

2 | HYBRID DISSIPATIVE TIME-VARYING DYNAMICAL SYSTEMS

This section aims to provide a sound base from which the desired passivity-based control design frameworks can be developed for hybrid nonlinear dynamical systems. In what is to follow, the preliminary definitions pertaining to the notion of dissipativity are first presented in Section 2.1. The hybrid nonlinear TV-KYP conditions, the significance of which is to characterize dissipativeness in terms of system dynamics and a generalized energy function, are then derived in Section 2.2. The results developed in Section 2.2 are then specialized to linear dynamical systems in Section 2.3. The feedback interconnection of hybrid dissipative dynamical systems is lastly discussed in Section 2.4.

Consider a hybrid dynamical system $\mathcal{G}$ modeled by nonlinear equations of the form:

$$\dot{\boldsymbol{x}}(t) = \boldsymbol{f}_{ct}(\boldsymbol{x}, t) + \boldsymbol{g}_{ct}(\boldsymbol{x}, t)\boldsymbol{u}_{ct}(t), \quad \boldsymbol{x}(t_0) = \boldsymbol{x}_0, \quad t \neq t_k, \tag{1}$$

$$\boldsymbol{y}_{ct}(t) = \boldsymbol{h}_{ct}(\boldsymbol{x}, t) + \boldsymbol{j}_{ct}(\boldsymbol{x}, t)\boldsymbol{u}_{ct}(t), \quad t \neq t_k, \tag{2}$$

$$\boldsymbol{x}_k^+ = \boldsymbol{f}_{ds}\left(\boldsymbol{x}_k^-, t\right) + \boldsymbol{g}_{ds}\left(\boldsymbol{x}_k^-, t\right)\boldsymbol{u}_{ds}(t), \quad t = t_k, \tag{3}$$

$$\boldsymbol{y}_{ds}(t) = \boldsymbol{h}_{ds}\left(\boldsymbol{x}_k^-, t\right) + \boldsymbol{j}_{ds}\left(\boldsymbol{x}_k^-, t\right)\boldsymbol{u}_{ds}(t), \quad t = t_k, \tag{4}$$

where $t \geq 0$, $\boldsymbol{x} \in \mathcal{D} \subseteq \mathbb{R}^n$ is the state vector, $\mathcal{D}$ specifies an open set with $\mathbf{0} \in \mathcal{D}$ defined as the state space of interest, $\boldsymbol{f}_{ct} : \mathcal{D} \times [0, \infty) \to \mathbb{R}^n$ is Lipschitz continuous on $\mathcal{D}$, $\boldsymbol{g}_{ct} : \mathcal{D} \times [0, \infty) \to \mathbb{R}^{n \times m_{ct}}$, $\boldsymbol{u}_{ct} \in \boldsymbol{U}_{ct} \subseteq \mathbb{R}^{m_{ct}}$ denotes the control input in the continuous-time subsystem, $\boldsymbol{y}_{ct} \in \boldsymbol{Y}_{ct} \subseteq \mathbb{R}^{q_{ct}}$ is the continuous-time output, $\boldsymbol{h}_{ct} : \mathcal{D} \times [0, \infty) \to \mathbb{R}^{q_{ct}}$, $\boldsymbol{j}_{ct} : \mathcal{D} \times [0, \infty) \to \mathbb{R}^{q_{ct} \times m_{ct}}$, and t_k indicates the time instants at which impulses are applied with $k \in \mathbb{Z}_{(t_0, t_f)} \triangleq \{k : t_0 < t_k < t_f\}$. Furthermore, $\boldsymbol{x}_k^- \triangleq \boldsymbol{x}\left(t_k^-\right)$ and $\boldsymbol{x}_k^+ \triangleq \boldsymbol{x}\left(t_k^+\right)$ denote, respectively, the state vector immediately before and after discrete-time dynamics are triggered at $t = t_k$, $\boldsymbol{f}_{ds} : \mathcal{D} \times [0, \infty) \to \mathbb{R}^n$ is continuous on $\mathcal{D}$, $\boldsymbol{g}_{ds} : \mathcal{D} \times [0, \infty) \to \mathbb{R}^{n \times m_{ds}}$, $\boldsymbol{u}_{ds} \in \boldsymbol{U}_{ds} \subseteq \mathbb{R}^{m_{ds}}$ specifies the discrete-time control input, $\boldsymbol{y}_{ds} \in \boldsymbol{Y}_{ds} \subseteq \mathbb{R}^{q_{ds}}$ is the discrete-time output, $\boldsymbol{h}_{ds} : \mathcal{D} \times [0, \infty) \to \mathbb{R}^{q_{ds}}$, and $\boldsymbol{j}_{ds} : \mathcal{D} \times [0, \infty) \to \mathbb{R}^{q_{ds} \times m_{ds}}$. It is also assumed that $(\boldsymbol{u}_{ct}(\cdot), \boldsymbol{u}_{ds}(\cdot))$ is restricted to the class of admissible control inputs $\mathcal{U} \triangleq \mathcal{U}_{ct} \times \mathcal{U}_{ds}$ consisting of measurable functions such that $(\boldsymbol{u}_{ct}, \boldsymbol{u}_{ds}) \in \boldsymbol{U}_{ct} \times \boldsymbol{U}_{ds}$ for all $t \geq 0$ and $k \in \mathbb{Z}_{(t_0, t_f)}$, where the constraint set $\boldsymbol{U} \triangleq \boldsymbol{U}_{ct} \times \boldsymbol{U}_{ds}$ is given with $(\mathbf{0}, \mathbf{0}) \in \boldsymbol{U}_{ct} \times \boldsymbol{U}_{ds}$. In addition, the required properties for the existence and uniqueness of solutions for (1) are presupposed to be satisfied such that (1) has a unique solution for all $t \in \mathbb{R}$.

2.1 | Preliminary definitions

Presenting the key definitions relevant to dissipativeness, this section paves the way for developing the TV-KYP conditions for hybrid nonlinear dynamical systems.

Definition 1. For the hybrid dynamical system $\mathcal{G}$ given by (1)–(4), a function $\left(S_{ct}\left(\boldsymbol{u}_{ct}, \boldsymbol{y}_{ct}\right), S_{ds}(\boldsymbol{u}_{ds}, \boldsymbol{y}_{ds})\right)$, where $S_{ct} : \boldsymbol{U}_{ct} \times \boldsymbol{Y}_{ct} \to \mathbb{R}$ and $S_{ds} : \boldsymbol{U}_{ds} \times \boldsymbol{Y}_{ds} \to \mathbb{R}$ are such that $S_{ct}(\mathbf{0}, \mathbf{0}) = 0$ and $S_{ds}(\mathbf{0}, \mathbf{0}) = 0$, is called a *hybrid supply rate* if, for all input–output pairs $\left(\boldsymbol{u}_{ct}, \boldsymbol{y}_{ct}\right) \in (\boldsymbol{U}_{ct}, \boldsymbol{Y}_{ct})$ and $\left(\boldsymbol{u}_{ds}, \boldsymbol{y}_{ds}\right) \in (\boldsymbol{U}_{ds}, \boldsymbol{Y}_{ds})$ satisfying (1)–(4) and for $k \in \mathbb{Z}_{(\tau_1, \tau_2)} \triangleq \{k : \tau_1 < t_k < \tau_2\}$, $S_{ct}\left(\boldsymbol{u}_{ct}, \boldsymbol{y}_{ct}\right)$ and $S_{ds}\left(\boldsymbol{u}_{ds}, \boldsymbol{y}_{ds}\right)$ benefit from the following properties:

$$\int_{\tau_1}^{\tau_2} \left| S_{ct}\left(\boldsymbol{u}_{ct}(t), \boldsymbol{y}_{ct}(t)\right) \right| \mathrm{d}t < \infty \quad \forall \tau_1, \tau_2 \geq 0, \tag{5}$$

$$\sum_{k \in \mathbb{Z}_{(\tau_1, \tau_2)}} \left| S_{ds}\left(\boldsymbol{u}_{ds}(t_k), \boldsymbol{y}_{ds}(t_k)\right) \right| < \infty, \tag{6}$$

Definition 2. The hybrid dynamical system $\mathcal{G}$ is *dissipative* with respect to the hybrid supply rate (S_{ct}, S_{ds}) if *the dissipation inequality* of the following form is satisfied for all $\tau \geq t_0$ and $(\boldsymbol{u}_{ct}(\cdot), \boldsymbol{u}_{ds}(\cdot)) \in \mathcal{U}_{ct} \times \mathcal{U}_{ds}$ with $\boldsymbol{x}(t_0) = \boldsymbol{0}$:

$$\int_{t_0}^{\tau} S_{ct}\left(\boldsymbol{u}_{ct}(t), \boldsymbol{y}_{ct}(t)\right) \mathrm{d}t + \sum_{k \in \mathbb{Z}_{(t_0,\tau)}} S_{ds}\left(\boldsymbol{u}_{ds}(t_k), \boldsymbol{y}_{ds}(t_k)\right) \geq 0, \tag{7}$$

Definition 3. The hybrid dynamical system $\mathcal{G}$ with $m_{ct} = q_{ct}$, $m_{ds} = q_{ds}$, and $\boldsymbol{x}(t_0) = \boldsymbol{0}$ is *passive* if

$$\int_{t_0}^{\tau} \boldsymbol{y}_{ct}^{\mathrm{T}}(t) \boldsymbol{u}_{ct}(t) \mathrm{d}t + \sum_{k \in \mathbb{Z}_{(t_0,\tau)}} \boldsymbol{y}_{ds}^{\mathrm{T}}(t_k)\, \boldsymbol{u}_{ds}(t_k) \geq 0 \tag{8}$$

for all $\tau \geq t_0$ and $(\boldsymbol{u}_{ct}(\cdot), \boldsymbol{u}_{ds}(\cdot)) \in \mathcal{U}_{ct} \times \mathcal{U}_{ds}$.

Equivalently, the hybrid dynamical system $\mathcal{G}$ with $m_{ct} = q_{ct}$ and $m_{ds} = q_{ds}$ is *passive* if $\mathcal{G}$ is dissipative with respect to a hybrid supply rate of the form $\left(S_{ct}\left(\boldsymbol{u}_{ct}, \boldsymbol{y}_{ct}\right), S_{ds}(\boldsymbol{u}_{ds}, \boldsymbol{y}_{ds})\right) = \left(2\boldsymbol{y}_{ct}^{\mathrm{T}}\boldsymbol{u}_{ct}, 2\boldsymbol{y}_{ds}^{\mathrm{T}}\boldsymbol{u}_{ds}\right)$.

Definition 4. The hybrid dynamical system $\mathcal{G}$ with $m_{ct} = q_{ct}$, $m_{ds} = q_{ds}$, and $\boldsymbol{x}(t_0) = \boldsymbol{0}$ is *input strictly passive* if there exist $\varepsilon_{ct} > 0$ and $\varepsilon_{ds} > 0$ such that

$$\int_{t_0}^{\tau} \boldsymbol{y}_{ct}^{\mathrm{T}}(t) \boldsymbol{u}_{ct}(t) \mathrm{d}t + \sum_{k \in \mathbb{Z}_{(t_0,\tau)}} \boldsymbol{y}_{ds}^{\mathrm{T}}(t_k)\, \boldsymbol{u}_{ds}(t_k) \geq \varepsilon_{ct} \int_{t_0}^{\tau} \boldsymbol{u}_{ct}^{\mathrm{T}}(t) \boldsymbol{u}_{ct}(t) \mathrm{d}t + \varepsilon_{ds} \sum_{k \in \mathbb{Z}_{(t_0,\tau)}} \boldsymbol{u}_{ds}^{\mathrm{T}}(t_k)\, \boldsymbol{u}_{ds}(t_k) \tag{9}$$

for all $\tau \geq t_0$ and $(\boldsymbol{u}_{ct}(\cdot), \boldsymbol{u}_{ds}(\cdot)) \in \mathcal{U}_{ct} \times \mathcal{U}_{ds}$.

Equivalently, the hybrid dynamical system $\mathcal{G}$ with $m_{ct} = q_{ct}$ and $m_{ds} = q_{ds}$ is *input strictly passive* if $\mathcal{G}$ is dissipative with respect to a hybrid supply rate of the form $\left(S_{ct}\left(\boldsymbol{u}_{ct}, \boldsymbol{y}_{ct}\right), S_{ds}(\boldsymbol{u}_{ds}, \boldsymbol{y}_{ds})\right) = \left(2\boldsymbol{y}_{ct}^{\mathrm{T}}\boldsymbol{u}_{ct} - 2\varepsilon_{ct}\boldsymbol{u}_{ct}^{\mathrm{T}}\boldsymbol{u}_{ct}, 2\boldsymbol{y}_{ds}^{\mathrm{T}}\boldsymbol{u}_{ds} - 2\varepsilon_{ds}\boldsymbol{u}_{ds}^{\mathrm{T}}\boldsymbol{u}_{ds}\right)$ where $\varepsilon_{ct} > 0$ and $\varepsilon_{ds} > 0$.

Definition 5. Consider the hybrid dynamical system $\mathcal{G}$ given by (1)–(4) with the hybrid supply rate (S_{ct}, S_{ds}). A continuous positive semi-definite function $V : \mathcal{D} \times \mathbb{R} \to \mathbb{R}$ satisfying $V(\boldsymbol{0}, t) = 0$ for all $t \in \mathbb{R}$ and

$$\int_{t_0}^{\tau} S_{ct}\left(\boldsymbol{u}_{ct}(t), \boldsymbol{y}_{ct}(t)\right) \mathrm{d}t + \sum_{k \in \mathbb{Z}_{(t_0,\tau)}} S_{ds}\left(\boldsymbol{u}_{ds}(t_k), \boldsymbol{y}_{ds}(t_k)\right) \geq V(\boldsymbol{x}(\tau), \tau) - V\left(\boldsymbol{x}(t_0), t_0\right) \tag{10}$$

is called a *storage function* for $\mathcal{G}$, where $\boldsymbol{x}(t)$ for $t \geq t_0$ is a solution to (1)–(4) with $(\boldsymbol{u}_{ct}(\cdot), \boldsymbol{u}_{ds}(\cdot)) \in \boldsymbol{U}_{ct} \times \boldsymbol{U}_{ds}$.

Definition 6. The hybrid dynamical system $\mathcal{G}$ is *completely reachable* if, for all $(\boldsymbol{x}_0, t_0) \in \mathcal{D} \times \mathbb{R}$, there exist a finite time $t_i \leq t_0$, square integrable input $\boldsymbol{u}_{ct}(t)$ defined on $[t_i, t_0]$, and input $\boldsymbol{u}_{ds}(t_k)$ defined on $k \in \mathbb{Z}_{(t_i,t_0)}$ such that the state $\boldsymbol{x}(t)$ for $t \geq t_i$ can be driven from $\boldsymbol{x}(t_i) = \boldsymbol{0}$ to $\boldsymbol{x}(t_0) = \boldsymbol{x}_0$.

With the key definitions thus in place, the notion of dissipativity for hybrid nonlinear dynamical systems can, now, be characterized in terms of inequalities involving generalized system power inputs, namely supply rates, and a generalized energy function, namely a storage function, as follows.

Theorem 1. *Assume the hybrid dynamical system $\mathcal{G}$ is completely reachable. $\mathcal{G}$ is then* dissipative *with respect to the hybrid supply rate (S_{ct}, S_{ds}) if and only if there exists a continuous positive semi-definite function $V : \mathcal{D} \times \mathbb{R} \to \mathbb{R}$ such that*

$$V\left(\boldsymbol{x}(\tau_2), \tau_2\right) - V\left(\boldsymbol{x}(\tau_1), \tau_1\right) \leq \int_{\tau_1}^{\tau_2} S_{ct}\left(\boldsymbol{u}_{ct}(t), \boldsymbol{y}_{ct}(t)\right) \mathrm{d}t, \quad t_k < \tau_1 \leq \tau_2 < t_{k+1}, \tag{11}$$

$$V\left(\boldsymbol{x}_k^+, t_k^+\right) - V\left(\boldsymbol{x}_k^-, t_k^-\right) \leq S_{ds}\left(\boldsymbol{u}_{ds}(t_k), \boldsymbol{y}_{ds}(t_k)\right), \quad k \in \mathbb{Z}_+, \tag{12}$$

where $\mathbb{Z}_+$ indicates the set of nonnegative integers and $V\left(\boldsymbol{x}_k^+, t_k^+\right) = V\left(\boldsymbol{f}_{ds} + \boldsymbol{g}_{ds}\boldsymbol{u}_{ds}, t_k^+\right)$.

Proof. Refer toHaddad et al.[1], Chapter 3 or Haddad et al.[19] ∎

The preceding theorem, in fact, obtains the necessary and sufficient conditions for dissipativity over an interval $t \in (t_k, t_{k+1})$ involving the consecutive impulsive instants t_k and t_{k+1}. Furthermore, the passive and input strictly passive dynamical systems can also be characterized via this theorem as dissipative systems with hybrid supply rates of a specific form.

The required tools are now in place to derive the TV-KYP conditions for hybrid nonlinear dynamical systems. This is the main objective of the next section.

2.2 | Hybrid nonlinear TV-KYP conditions

This section serves to characterize passivity and input strict passivity, as special cases of dissipativity, for $\mathcal{G}$ in terms of the system functions and the storage function $V(\boldsymbol{x}, t)$ via the TV-KYP conditions.

Theorem 2. *Consider the hybrid dynamical system $\mathcal{G}$ with $m_{ct} = q_{ct}$, $m_{ds} = q_{ds}$, $\mathcal{D} = \mathbb{R}^n$, $\boldsymbol{U}_{ct} = \mathbb{R}^{m_{ct}}$, $\boldsymbol{Y}_{ct} = \mathbb{R}^{q_{ct}}$, $\boldsymbol{U}_{ds} = \mathbb{R}^{m_{ds}}$, and $\boldsymbol{Y}_{ds} = \mathbb{R}^{q_{ds}}$. Furthermore, assume that the dynamical properties of the system in question evolve periodically over time. If there exist functions $V : \mathbb{R}^n \times [0, \infty) \to \mathbb{R}$, $\boldsymbol{l}_{ct} : \mathbb{R}^n \times [0, \infty) \to \mathbb{R}^{p_{ct}}$, $\boldsymbol{w}_{ct} : \mathbb{R}^n \times [0, \infty) \to \mathbb{R}^{p_{ct} \times m_{ct}}$, $\boldsymbol{l}_{ds} : \mathbb{R}^n \times [0, \infty) \to \mathbb{R}^{p_{ds}}$, and $\boldsymbol{w}_{ds} : \mathbb{R}^n \times \mathbb{R} \to \mathbb{R}^{p_{ds} \times m_{ds}}$ such that (I) $V(\boldsymbol{x}, t)$ is continuously differentiable and positive definite, (II) $V(\boldsymbol{0}, t) = 0$, (III) the storage function in the discrete-time subsystem is structurally constrained to conform to*

$$\begin{aligned} V\left(\boldsymbol{x}_k^+, t_k^+\right) &= V\left(\boldsymbol{f}_{ds} + \boldsymbol{g}_{ds}\boldsymbol{u}_{ds}, t_k^+\right) \\ &= V\left(\boldsymbol{f}_{ds}, t_k^+\right) + \boldsymbol{\mathcal{R}}'_{\boldsymbol{u}_{ds}}(\boldsymbol{x}_k, t_k)\,\boldsymbol{u}_{ds}(t_k) + \boldsymbol{u}_{ds}^{\mathrm{T}}(t_k)\,\boldsymbol{\mathcal{R}}''_{\boldsymbol{u}_{ds}}(\boldsymbol{x}_k, t_k)\,\boldsymbol{u}_{ds}(t_k), \end{aligned} \tag{13}$$

where

$$\boldsymbol{\mathcal{R}}'_{\boldsymbol{u}_{ds}}(\boldsymbol{x}_k, t_k) = \left.\frac{\partial V\left(\boldsymbol{f}_{ds} + \boldsymbol{g}_{ds}\boldsymbol{u}_{ds}, t_k^+\right)}{\partial \boldsymbol{u}_{ds}^{\mathrm{T}}}\right|_{\boldsymbol{u}_{ds}=\boldsymbol{0}} = \left(\frac{\partial V\left(\boldsymbol{f}_{ds}, t_k^+\right)}{\partial \boldsymbol{x}}\right)^{\mathrm{T}} \boldsymbol{g}_{ds}, \tag{14}$$

$$\boldsymbol{\mathcal{R}}''_{\boldsymbol{u}_{ds}}(\boldsymbol{x}_k, t_k) = \left.\frac{\partial^2 V\left(\boldsymbol{f}_{ds} + \boldsymbol{g}_{ds}\boldsymbol{u}_{ds}, t_k^+\right)}{\partial \boldsymbol{u}_{ds}\partial \boldsymbol{u}_{ds}^{\mathrm{T}}}\right|_{\boldsymbol{u}_{ds}=\boldsymbol{0}} = \frac{1}{2}\boldsymbol{g}_{ds}^{\mathrm{T}}\frac{\partial^2 V\left(\boldsymbol{f}_{ds}, t_k^+\right)}{\partial \boldsymbol{x}\partial \boldsymbol{x}^{\mathrm{T}}}\boldsymbol{g}_{ds} \tag{15}$$

for all $\boldsymbol{x} \in \mathbb{R}^n$ and $\boldsymbol{u}_{ds} \in \mathbb{R}^{m_{ds}}$, and (IV) continuous-time and discrete-time sets of equations of the form

$$\frac{\partial V(\boldsymbol{x}, t)}{\partial t} + \left(\frac{\partial V(\boldsymbol{x}, t)}{\partial \boldsymbol{x}}\right)^{\mathrm{T}} \boldsymbol{f}_{ct}(\boldsymbol{x}, t) + \boldsymbol{l}_{ct}^{\mathrm{T}}(\boldsymbol{x}, t)\boldsymbol{l}_{ct}(\boldsymbol{x}, t) = 0, \tag{16}$$

$$\frac{1}{2}\left(\frac{\partial V(\boldsymbol{x}, t)}{\partial \boldsymbol{x}}\right)^{\mathrm{T}} \boldsymbol{g}_{ct}(\boldsymbol{x}, t) - \boldsymbol{h}_{ct}^{\mathrm{T}}(\boldsymbol{x}, t) + \boldsymbol{l}_{ct}^{\mathrm{T}}(\boldsymbol{x}, t)\boldsymbol{w}_{ct}(\boldsymbol{x}, t) = \boldsymbol{0}, \tag{17}$$

$$-2\varepsilon_{ct}\boldsymbol{1}_{m_{ct} \times m_{ct}} + \boldsymbol{j}_{ct}(\boldsymbol{x}, t) + \boldsymbol{j}_{ct}^{\mathrm{T}}(\boldsymbol{x}, t) - \boldsymbol{w}_{ct}^{\mathrm{T}}(\boldsymbol{x}, t)\boldsymbol{w}_{ct}(\boldsymbol{x}, t) = \boldsymbol{0}, \tag{18}$$

$$V\left(\boldsymbol{f}_{ds}, t_k^+\right) - V\left(\boldsymbol{x}_k^-, t_k^-\right) + \boldsymbol{l}_{ds}^{\mathrm{T}}(\boldsymbol{x}_k, t_k)\,\boldsymbol{l}_{ds}(\boldsymbol{x}_k, t_k) = 0, \tag{19}$$

$$\frac{1}{2}\boldsymbol{\mathcal{R}}'_{\boldsymbol{u}_{ds}}(\boldsymbol{x}_k, t_k) - \boldsymbol{h}_{ds}^{\mathrm{T}}(\boldsymbol{x}_k, t_k) + \boldsymbol{l}_{ds}^{\mathrm{T}}(\boldsymbol{x}_k, t_k)\,\boldsymbol{w}_{ds}(\boldsymbol{x}_k, t_k) = \boldsymbol{0}, \tag{20}$$

$$-2\varepsilon_{ds}\boldsymbol{1}_{m_{ds} \times m_{ds}} + \boldsymbol{j}_{ds}(\boldsymbol{x}_k, t_k) + \boldsymbol{j}_{ds}^{\mathrm{T}}(\boldsymbol{x}_k, t_k) - \boldsymbol{\mathcal{R}}''_{\boldsymbol{u}_{ds}}(\boldsymbol{x}_k, t_k) - \boldsymbol{w}_{ds}^{\mathrm{T}}(\boldsymbol{x}_k, t_k)\,\boldsymbol{w}_{ds}(\boldsymbol{x}_k, t_k) = \boldsymbol{0}, \tag{21}$$

are fulfilled for $\varepsilon_{ct} \geq 0$, $\varepsilon_{ds} \geq 0$, and all $\boldsymbol{x} \in \mathbb{R}^n$; the hybrid dynamical system $\mathcal{G}$ is then passive *if $\varepsilon_{ct} = \varepsilon_{ds} \equiv 0$, and is* input strictly passive *if $\varepsilon_{ct} > 0$ and $\varepsilon_{ds} > 0$.*

Proof. For any admissible control input $\boldsymbol{u}_{ct}(t)$, where $\tau_1, \tau_2 \in [0, \infty)$, $t_k < \tau_1 \leq \tau_2 < t_{k+1}$, and $k \in \mathbb{Z}_+$, (16)–(18) imply

$$\begin{aligned} V(\boldsymbol{x}(\tau_2), \tau_2) - V(\boldsymbol{x}(\tau_1), \tau_1) &= \int_{\tau_1}^{\tau_2} \dot{V}(\boldsymbol{x}(t), t)\mathrm{d}t \\ &\leq \int_{\tau_1}^{\tau_2} \left(\dot{V}(\boldsymbol{x}, t) + (\boldsymbol{l}_{ct} + \boldsymbol{w}_{ct}\boldsymbol{u}_{ct})^{\mathrm{T}}(\boldsymbol{l}_{ct} + \boldsymbol{w}_{ct}\boldsymbol{u}_{ct})\right) \mathrm{d}t \end{aligned}$$

$$
\begin{aligned}
&= \int_{\tau_1}^{\tau_2} \left(\partial V/\partial t + (\partial V/\partial \boldsymbol{x})^{\mathrm{T}}\dot{\boldsymbol{x}} + \boldsymbol{l}_{ct}^{\mathrm{T}}\boldsymbol{l}_{ct} + \boldsymbol{u}_{ct}^{\mathrm{T}}\boldsymbol{w}_{ct}^{\mathrm{T}}\boldsymbol{w}_{ct}\boldsymbol{u}_{ct} + 2\boldsymbol{l}_{ct}^{\mathrm{T}}\boldsymbol{w}_{ct}\boldsymbol{u}_{ct}\right) \mathrm{d}t \\
&= \int_{\tau_1}^{\tau_2} \left(\partial V/\partial t + (\partial V/\partial \boldsymbol{x})^{\mathrm{T}}\boldsymbol{f}_{ct} + \underbrace{(\partial V/\partial \boldsymbol{x})^{\mathrm{T}}\boldsymbol{g}_{ct}}_{(16)}\boldsymbol{u}_{ct} + \underbrace{\boldsymbol{l}_{ct}^{\mathrm{T}}\boldsymbol{l}_{ct}}_{(15)} + \boldsymbol{u}_{ct}^{\mathrm{T}}\underbrace{\boldsymbol{w}_{ct}^{\mathrm{T}}\boldsymbol{w}_{ct}}_{(17)}\boldsymbol{u}_{ct} + 2\boldsymbol{l}_{ct}^{\mathrm{T}}\boldsymbol{w}_{ct}\boldsymbol{u}_{ct}\right) \mathrm{d}t \\
&= \int_{\tau_1}^{\tau_2} \Big(\cancel{\partial V/\partial t} + \cancel{(\partial V/\partial \boldsymbol{x})^{\mathrm{T}}\boldsymbol{f}_{ct}} + 2\boldsymbol{h}_{ct}^{\mathrm{T}}\boldsymbol{u}_{ct} - \cancel{2\boldsymbol{l}_{ct}^{\mathrm{T}}\boldsymbol{w}_{ct}\boldsymbol{u}_{ct}} \\
&\quad \cancel{-\partial V/\partial t} - \cancel{(\partial V/\partial \boldsymbol{x})^{\mathrm{T}}\boldsymbol{f}_{ct}} - 2\varepsilon_{ct}\boldsymbol{u}_{ct}^{\mathrm{T}}\boldsymbol{u}_{ct} + \boldsymbol{u}_{ct}^{\mathrm{T}}\boldsymbol{j}_{ct}\boldsymbol{u}_{ct} + \boldsymbol{u}_{ct}^{\mathrm{T}}\boldsymbol{j}_{ct}^{\mathrm{T}}\boldsymbol{u}_{ct} + \cancel{2\boldsymbol{l}_{ct}^{\mathrm{T}}\boldsymbol{w}_{ct}\boldsymbol{u}_{ct}}\Big) \mathrm{d}t \\
&= \int_{\tau_1}^{\tau_2} \left(2\boldsymbol{h}_{ct}^{\mathrm{T}}\boldsymbol{u}_{ct} + 2\boldsymbol{u}_{ct}^{\mathrm{T}}\boldsymbol{j}_{ct}^{\mathrm{T}}\boldsymbol{u}_{ct} - 2\varepsilon_{ct}\boldsymbol{u}_{ct}^{\mathrm{T}}\boldsymbol{u}_{ct}\right) \mathrm{d}t = \int_{\tau_1}^{\tau_2} \left(2\boldsymbol{y}_{ct}^{\mathrm{T}}\boldsymbol{u}_{ct} - 2\varepsilon_{ct}\boldsymbol{u}_{ct}^{\mathrm{T}}\boldsymbol{u}_{ct}\right) \mathrm{d}t = \int_{\tau_1}^{\tau_2} S_{ct}\left(\boldsymbol{u}_{ct}, \boldsymbol{y}_{ct}\right) \mathrm{d}t,
\end{aligned}
\tag{22}
$$

where $\boldsymbol{x}(t)$, $t \in (t_k, t_{k+1})$, satisfies (1) and $\dot{V}(\cdot)$ denotes the total derivative of the storage function along the trajectories $\boldsymbol{x}(t)$ of (1). Therefore: $V\left(\boldsymbol{x}(\tau_2), \tau_2\right) - V\left(\boldsymbol{x}(\tau_1), \tau_1\right) \leq \int_{\tau_1}^{\tau_2} S_{ct}\left(\boldsymbol{u}_{ct}, \boldsymbol{y}_{ct}\right) \mathrm{d}t$. ∎

Next, for any admissible control input $\boldsymbol{u}_{ds}(t_k)$, where $t_k \in \mathbb{R}$ and $k \in \mathbb{Z}_+$, it follows from (13)–(15) along with (19)–(21) that for all $\boldsymbol{x} \in \mathbb{R}^n$ and $\boldsymbol{u}_{ds} \in \mathbb{R}^{m_{ds}}$:

$$
\begin{aligned}
\Delta V(\boldsymbol{x}_k, t_k) &= V\left(\boldsymbol{x}_k^+, t_k^+\right) - V\left(\boldsymbol{x}_k^-, t_k^-\right) \\
&= \underbrace{V\left(\boldsymbol{f}_{ds} + \boldsymbol{g}_{ds}\boldsymbol{u}_{ds}, t_k^+\right)}_{(12)-(14)} - V\left(\boldsymbol{x}_k^-, t_k^-\right) \\
&= \underbrace{V\left(\boldsymbol{f}_{ds}, t_k^+\right) - V\left(\boldsymbol{x}_k^-, t_k^-\right)}_{(18)} + \underbrace{\mathcal{R}'_{\boldsymbol{u}_{ds}}\boldsymbol{u}_{ds}}_{(19)} + \boldsymbol{u}_{ds}^{\mathrm{T}}\underbrace{\mathcal{R}''_{\boldsymbol{u}_{ds}}}_{(20)}\boldsymbol{u}_{ds} \\
&= -\boldsymbol{l}_{ds}^{\mathrm{T}}\boldsymbol{l}_{ds} + 2\boldsymbol{h}_{ds}^{\mathrm{T}}\boldsymbol{u}_{ds} - 2\boldsymbol{l}_{ds}^{\mathrm{T}}\boldsymbol{w}_{ds}\boldsymbol{u}_{ds} - 2\varepsilon_{ds}\boldsymbol{u}_{ds}^{\mathrm{T}}\boldsymbol{u}_{ds} + \boldsymbol{u}_{ds}^{\mathrm{T}}\boldsymbol{j}_{ds}\boldsymbol{u}_{ds} + \boldsymbol{u}_{ds}^{\mathrm{T}}\boldsymbol{j}_{ds}^{\mathrm{T}}\boldsymbol{u}_{ds} - \boldsymbol{u}_{ds}^{\mathrm{T}}\boldsymbol{w}_{ds}^{\mathrm{T}}\boldsymbol{w}_{ds}\boldsymbol{u}_{ds} \\
&= \left(2\boldsymbol{h}_{ds}^{\mathrm{T}}\boldsymbol{u}_{ds} + 2\boldsymbol{u}_{ds}^{\mathrm{T}}\boldsymbol{j}_{ds}^{\mathrm{T}}\boldsymbol{u}_{ds} - 2\varepsilon_{ds}\boldsymbol{u}_{ds}^{\mathrm{T}}\boldsymbol{u}_{ds}\right) - \left(\boldsymbol{l}_{ds}^{\mathrm{T}}\boldsymbol{l}_{ds} + 2\boldsymbol{l}_{ds}^{\mathrm{T}}\boldsymbol{w}_{ds}\boldsymbol{u}_{ds} + \boldsymbol{u}_{ds}^{\mathrm{T}}\boldsymbol{w}_{ds}^{\mathrm{T}}\boldsymbol{w}_{ds}\boldsymbol{u}_{ds}\right) \\
&= \left(2\boldsymbol{y}_{ds}^{\mathrm{T}}\boldsymbol{u}_{ds} - 2\varepsilon_{ds}\boldsymbol{u}_{ds}^{\mathrm{T}}\boldsymbol{u}_{ds}\right) - \left(\boldsymbol{l}_{ds} + \boldsymbol{w}_{ds}\boldsymbol{u}_{ds}\right)^{\mathrm{T}}\left(\boldsymbol{l}_{ds} + \boldsymbol{w}_{ds}\boldsymbol{u}_{ds}\right) \\
&= S_{ds}\left(\boldsymbol{u}_{ds}, \boldsymbol{y}_{ds}\right) - \left(\boldsymbol{l}_{ds} + \boldsymbol{w}_{ds}\boldsymbol{u}_{ds}\right)^{\mathrm{T}}\left(\boldsymbol{l}_{ds} + \boldsymbol{w}_{ds}\boldsymbol{u}_{ds}\right) \\
&\leq S_{ds}\left(\boldsymbol{u}_{ds}, \boldsymbol{y}_{ds}\right),
\end{aligned}
\tag{23}
$$

where $\Delta V(\cdot)$ denotes the difference of the storage function at the impulsive instants t_k of (3).

Since a hybrid supply rate of the form $(S_{ct}, S_{ds}) = \left(2\boldsymbol{y}_{ct}^{\mathrm{T}}\boldsymbol{u}_{ct} - 2\varepsilon_{ct}\boldsymbol{u}_{ct}^{\mathrm{T}}\boldsymbol{u}_{ct}, 2\boldsymbol{y}_{ds}^{\mathrm{T}}\boldsymbol{u}_{ds} - 2\varepsilon_{ds}\boldsymbol{u}_{ds}^{\mathrm{T}}\boldsymbol{u}_{ds}\right)$ corresponds to passivity when $\varepsilon_{ct} = \varepsilon_{ds} \equiv 0$ and to input strict passivity when $\varepsilon_{ct} > 0$ and $\varepsilon_{ds} > 0$; in view of (22) and (23), the proof is now complete in accordance with Theorem 1.

2.3 | Hybrid linear TV-KYP conditions

In this section, the TV-KYP conditions developed in the preceding section are specialized to hybrid linear dynamical systems. Defining $\boldsymbol{x}_{eq} = \boldsymbol{0}$ as desired operating points for the linearization, the hybrid nonlinear dynamical system represented by (1)–(4) can be linearized as follows:

$$
\dot{\boldsymbol{x}}(t) = \boldsymbol{A}_{ct}(t)\boldsymbol{x} + \boldsymbol{B}_{ct}(t)\boldsymbol{u}_{ct}(t), \quad \boldsymbol{x}(t_0) = \boldsymbol{x}_0, \quad t \neq t_k, \tag{24}
$$

$$
\boldsymbol{y}_{ct}(t) = \boldsymbol{C}_{ct}(t)\boldsymbol{x} + \boldsymbol{D}_{ct}(t)\boldsymbol{u}_{ct}(t), \quad t \neq t_k, \tag{25}
$$

$$
\boldsymbol{x}_k^+ = \boldsymbol{A}_{ds}(t)\boldsymbol{x}_k^- + \boldsymbol{B}_{ds}(t)\boldsymbol{u}_{ds}(t), \quad t = t_k, \tag{26}
$$

$$
\boldsymbol{y}_{ds}(t) = \boldsymbol{C}_{ds}(t)\boldsymbol{x}_k^- + \boldsymbol{D}_{ds}(t)\boldsymbol{u}_{ds}(t), \quad t = t_k, \tag{27}
$$

where $\boldsymbol{A}_{ct} = \mathbf{J}_{\boldsymbol{x}}\left(\boldsymbol{f}_{ct}\right)\big|_{\boldsymbol{x}=\boldsymbol{x}_{eq}} \in \mathbb{R}^{n\times n}$, $\boldsymbol{B}_{ct} = \boldsymbol{g}_{ct}\big|_{\boldsymbol{x}=\boldsymbol{x}_{eq}} \in \mathbb{R}^{n\times m_{ct}}$, $\boldsymbol{C}_{ct} = \mathbf{J}_{\boldsymbol{x}}(\boldsymbol{h}_{ct})|_{\boldsymbol{x}=\boldsymbol{x}_{eq}} \in \mathbb{R}^{q_{ct}\times n}$, and $\boldsymbol{D}_{ct} = \boldsymbol{j}_{ct}\big|_{\boldsymbol{x}=\boldsymbol{x}_{eq}} \in \mathbb{R}^{q_{ct}\times m_{ct}}$ along with $\boldsymbol{A}_{ds} = \mathbf{J}_{\boldsymbol{x}}\left(\boldsymbol{f}_{ds}\right)\big|_{\boldsymbol{x}=\boldsymbol{x}_{eq}} \in \mathbb{R}^{n\times n}$, $\boldsymbol{B}_{ds} = \boldsymbol{g}_{ds}\big|_{\boldsymbol{x}=\boldsymbol{x}_{eq}} \in \mathbb{R}^{n\times m_{ds}}$, $\boldsymbol{C}_{ds} = \mathbf{J}_{\boldsymbol{x}}(\boldsymbol{h}_{ds})|_{\boldsymbol{x}=\boldsymbol{x}_{eq}} \in \mathbb{R}^{q_{ds}\times n}$, and $\boldsymbol{D}_{ds} = \boldsymbol{j}_{ds}\big|_{\boldsymbol{x}=\boldsymbol{x}_{eq}} \in \mathbb{R}^{q_{ds}\times m_{ds}}$ define the time-dependent system matrices associated with continuous-time and

discrete-time subsystems, respectively, and $\mathbf{J}_{\boldsymbol{x}}$ denotes the Jacobian matrix with respect to $\boldsymbol{x}$. The hybrid TV-KYP conditions characterizing passivity and input strict passivity for hybrid linear dynamical systems can, now, be presented as follows.

Corollary 1. *Consider the linearized hybrid dynamical system described by (25)–(27) with $m_{ct} = q_{ct}$ and $m_{ds} = q_{ds}$. Furthermore, assume the dynamical properties of the system being considered evolve periodically over time. If there exist matrices $\boldsymbol{P} = \boldsymbol{P}^{\mathrm{T}} \in \mathbb{R}^{n\times n} > \mathbf{0}$, $\boldsymbol{L}_{ct} \in \mathbb{R}^{p_{ct}\times n}$, $\boldsymbol{W}_{ct} \in \mathbb{R}^{p_{ct}\times m_{ct}}$, $\boldsymbol{L}_{ds} \in \mathbb{R}^{p_{ds}\times n}$, and $\boldsymbol{W}_{ds} \in \mathbb{R}^{p_{ds}\times m_{ds}}$ such that continuous-time and discrete-time equations of the form*

$$\dot{\boldsymbol{P}}(t) + \boldsymbol{A}_{ct}^{\mathrm{T}}(t)\boldsymbol{P}(t) + \boldsymbol{P}(t)\boldsymbol{A}_{ct}(t) + \boldsymbol{L}_{ct}^{\mathrm{T}}(t)\boldsymbol{L}_{ct}(t) = \mathbf{0}, \tag{28}$$

$$\boldsymbol{P}(t)\boldsymbol{B}_{ct}(t) - \boldsymbol{C}_{ct}^{\mathrm{T}}(t) + \boldsymbol{L}_{ct}^{\mathrm{T}}(t)\boldsymbol{W}_{ct}(t) = \mathbf{0}, \tag{29}$$

$$-2\varepsilon_{ct}\mathbf{1}_{m_{ct}\times m_{ct}} + \boldsymbol{D}_{ct}(t) + \boldsymbol{D}_{ct}^{\mathrm{T}}(t) - \boldsymbol{W}_{ct}^{\mathrm{T}}(t)\boldsymbol{W}_{ct}(t) = \mathbf{0}, \tag{30}$$

$$\boldsymbol{A}_{ds}^{\mathrm{T}}(t_k)\,\boldsymbol{P}\left(t_k^{+}\right)\boldsymbol{A}_{ds}(t_k) - \boldsymbol{P}\left(t_k^{-}\right) + \boldsymbol{L}_{ds}^{\mathrm{T}}(t_k)\,\boldsymbol{L}_{ds}(t_k) = \mathbf{0}, \tag{31}$$

$$\boldsymbol{A}_{ds}^{\mathrm{T}}(t_k)\,\boldsymbol{P}\left(t_k^{+}\right)\boldsymbol{B}_{ds}(t_k) - \boldsymbol{C}_{ds}^{\mathrm{T}}(t_k) + \boldsymbol{L}_{ds}^{\mathrm{T}}(t_k)\,\boldsymbol{W}_{ds}(t_k) = \mathbf{0}, \tag{32}$$

$$-2\varepsilon_{ds}\mathbf{1}_{m_{ds}\times m_{ds}} + \boldsymbol{D}_{ds}(t_k) + \boldsymbol{D}_{ds}^{\mathrm{T}}(t_k) - \boldsymbol{B}_{ds}^{\mathrm{T}}(t_k)\,\boldsymbol{P}\left(t_k^{+}\right)\boldsymbol{B}_{ds}(t_k) - \boldsymbol{W}_{ds}^{\mathrm{T}}(t_k)\,\boldsymbol{W}_{ds}(t_k) = \mathbf{0} \tag{33}$$

are met; the linearized dynamical system is passive *if $\varepsilon_{ct} = \varepsilon_{ds} \equiv 0$, and is* input strictly passive *if $\varepsilon_{ct} > 0$ and $\varepsilon_{ds} > 0$.*

Proof. The result is a direct consequence of Theorem 2 by setting $V(\boldsymbol{x}, t) = \boldsymbol{x}^{\mathrm{T}}\boldsymbol{P}(t)\boldsymbol{x}$, $\boldsymbol{f}_{ct} = \boldsymbol{A}_{ct}\boldsymbol{x}$, $\boldsymbol{g}_{ct} = \boldsymbol{B}_{ct}$, $\boldsymbol{h}_{ct} = \boldsymbol{C}_{ct}\boldsymbol{x}$, $\boldsymbol{j}_{ct} = \boldsymbol{D}_{ct}$, $\boldsymbol{f}_{ds} = \boldsymbol{A}_{ds}\boldsymbol{x}_k^-$, $\boldsymbol{g}_{ds} = \boldsymbol{B}_{ds}$, $\boldsymbol{h}_{ds} = \boldsymbol{C}_{ds}\boldsymbol{x}_k^-$, $\boldsymbol{j}_{ds} = \boldsymbol{D}_{ds}$, $\boldsymbol{l}_{ct} = \boldsymbol{L}_{ct}\boldsymbol{x}$, $\boldsymbol{w}_{ct} = \boldsymbol{W}_{ct}$, $\boldsymbol{l}_{ds} = \boldsymbol{L}_{ds}\boldsymbol{x}$, and $\boldsymbol{w}_{ds} = \boldsymbol{W}_{ds}$. ∎

2.4 | Feedback interconnection of hybrid dissipative systems

Placing the passivity theorem (Refer to Reference 9 for the original form and to Reference 32 for the extended hybrid version) as a solid foundation, this section aims to discuss feedback interconnection of hybrid dissipative dynamical systems to construct stable closed-loop dynamics. Figure 1 shows a schematic representation of how two hybrid dynamical systems, namely a plant $\mathcal{G}$ and a controller $\mathcal{H}$, are interconnected through negative feedback to establish a closed-loop system under the influence of hybrid external disturbances $(\boldsymbol{d}_{ct}, \boldsymbol{d}_{ds})$, where $(\boldsymbol{u}_{ct}, \boldsymbol{u}_{ds,k})$ is the hybrid input of the plant to be controlled with $\boldsymbol{u}_{ds,k} \triangleq \boldsymbol{u}_{ds}(\boldsymbol{x}(t_k), t_k)$; $(\boldsymbol{y}_{ct}, \boldsymbol{y}_{ds})$ defines the hybrid output of the plant; $(\widehat{\boldsymbol{u}}_{ct}, \widehat{\boldsymbol{u}}_{ds,k})$ represents the hybrid input of the controller with $\widehat{\boldsymbol{u}}_{ds,k} \triangleq \widehat{\boldsymbol{u}}_{ds}(\widehat{\boldsymbol{x}}(t_k), t_k)$, which is equal to $(\boldsymbol{y}_{ct}, \boldsymbol{y}_{ds})$ when measurement noise is negligible; and $(\widehat{\boldsymbol{y}}_{ct}, \widehat{\boldsymbol{y}}_{ds})$ specifies the hybrid output of the controller. In accordance with the passivity theorem, the negative feedback interconnection of a passive system and an input strictly passive system is input–output stable. Figure 1 can, therefore, be used to illuminate the passivity theorem further as follows: passivity of the hybrid plant $\mathcal{G}$ and input strict passivity of the hybrid controller $\mathcal{H}$ imply input–output stability of the closed-loop system through a negative feedback interconnection.

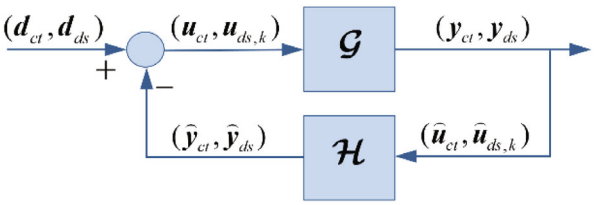

FIGURE 1 Schematic representation of closed-loop system composed of hybrid plant $\mathcal{G}$ and hybrid controller $\mathcal{H}$.

3 | PASSIVITY-BASED CONTROL

Utilizing the TV-KYP conditions developed in Section 2 in tandem with the passivity theorem, this section presents a three-step control design procedure to derive the passivity-based control design frameworks in question. In this regard, the hybrid output dynamics of the plant are judiciously determined in the first step to satisfy the passivity specifications via the passivity-related TV-KYP conditions represented by (16)–(21) with $\varepsilon_{ct} = \varepsilon_{ds} \equiv 0$. A hybrid control scheme, which separately adopts compensators of static and dynamic structures in the feedback path, is then designed to meet the input strict passivity requirements. The stability of the closed-loop system is consequently established by a negative feedback interconnection between the resultant hybrid plant and controller.

To pursue the first objective, (16) and (19) must be solved simultaneously for $V(\boldsymbol{x}, t)$ in an interacting manner. These equations are, however, difficult to solve in general, thereby necessitating approximation techniques. Aiming to rise to this challenge, a hybrid computational framework involving two numerical schemes pertaining to the continuous-time and discrete-time subsystems is therefore proposed in the following subsections to approximate the storage function in each continuous-time and discrete time subsystem. The hybrid output dynamics of the plant satisfying passivity properties from input to output can, subsequently, be determined in terms of $V(\boldsymbol{x}, t)$ through the remaining conditions, that is, (17), (18), (20), and (21) with $\varepsilon_{ct} = \varepsilon_{ds} \equiv 0$.

3.1 | Numerical solution to differential TV-KYP equation

Employing the Galerkin spectral method,[33] a set of ordinary differential equations is derived in this section to numerically solve the differential TV-KYP equation, (16), thereby approximating the storage function between impulsive events. The basic idea underlying the Galerkin-based approximation is to assume that the solution to (16), i.e. the storage function, can be expressed as an infinite sum of known basis functions. Furthermore, in order for the Galerkin spectral method to be applicable, the resultant formulation must be placed in a suitable inner product space such that the projection is well-defined in terms of n-dimensional integrations. The approximation is thus restricted to a closed and bounded set in $\boldsymbol{\mathcal{D}}$, namely a compact set $\boldsymbol{\Omega}$, which defines the bounded domain of the state space of interest. Therefore, it is first assumed that the storage function in (16) can be discretized by an infinite series of prescribed state-dependent basis functions, which are continuous and defined everywhere on $\boldsymbol{\Omega}$, and unknown coefficients with time-dependency as follows:

$$V(\boldsymbol{x}, t) \coloneqq \sum_{j=1}^{\infty} c_j(t)\phi_j(\boldsymbol{x}). \tag{34}$$

Nevertheless, from a practical point of view, using an infinite number of terms for discretizing the abovementioned quantity is impossible; the approximation process for $V(\boldsymbol{x}, t)$ continues further with considering a truncated version of the infinite series represented by (34) involving the first N terms:

$$V_N(\boldsymbol{x}, t) \coloneqq \sum_{j=1}^{N} c_j(t)\phi_j(\boldsymbol{x}) = \boldsymbol{\Phi}_N^{\mathrm{T}}(\boldsymbol{x})\boldsymbol{C}_N(t), \tag{35}$$

where $\boldsymbol{\Phi}_N(\boldsymbol{x}) = [\phi_1(\boldsymbol{x}) \ \dots \ \phi_N(\boldsymbol{x})]^{\mathrm{T}}$ denotes a prescribed state-dependent set of basis functions, $\boldsymbol{C}_N(t) = [c_1(t) \ \dots \ c_N(t)]^{\mathrm{T}}$ specifies the corresponding collection of unknown time-dependent coefficients, and N refers to the number of basis elements (i.e., the order of approximation). The approximation sequence then proceeds with substituting (35) into (16), which, in turn, results in an error equation due primarily to approximating the storage function with $V_N(\boldsymbol{x}, t)$. Utilizing the Galerkin spectral method, the unknown coefficients, $\boldsymbol{C}_N(t)$, are therefore determined such that the resultant error is minimized. To this end, the error equation is projected onto the same basis functions retained in the truncated series and the outcome is set equal to zero so as to obtain N simultaneous equations for N unknowns:

$$\left\langle \underset{\textit{differential}}{\text{TV-KYP}}\left(\sum_{j=1}^{N} c_j(t)\phi_j(\boldsymbol{x})\right), \boldsymbol{\Phi}_N(\boldsymbol{x}) \right\rangle_{\boldsymbol{\Omega}} = \boldsymbol{0}, \tag{36}$$

where the projection operator is the inner product $\langle(\cdot), \phi_i(\boldsymbol{x})\rangle_{\boldsymbol{\Omega}} \triangleq \int_{\boldsymbol{\Omega}}(\cdot)\phi_i(\boldsymbol{x})\mathrm{d}\boldsymbol{x}$ computed over a closed and bounded set, $\boldsymbol{\Omega}$. The preceding set of equations represents the Galerkin-based projection of the differential TV-KYP equation in a compact form, which can be expanded as follows:

$$\langle \boldsymbol{\Phi}_N, \boldsymbol{\Phi}_N\rangle_{\boldsymbol{\Omega}}\, \dot{\boldsymbol{C}}_N(t) + \left\langle \mathbf{J}_{\boldsymbol{x}}(\boldsymbol{\Phi}_N)\boldsymbol{f}_{ct}, \boldsymbol{\Phi}_N\right\rangle_{\boldsymbol{\Omega}} \boldsymbol{C}_N(t) + \left\langle \boldsymbol{l}_{ct}^{\mathrm{T}}\boldsymbol{l}_{ct}, \boldsymbol{\Phi}_N\right\rangle_{\boldsymbol{\Omega}} = \mathbf{0}. \tag{37}$$

Considering $\boldsymbol{l}_{ct}(\boldsymbol{x}, t)$ as a design parameter to be appropriately selected by the user, the following set of ordinary differential equations termed *the continuous-time passivity-based control gain equations* needs therefore to be integrated backward in time in order to compute $\boldsymbol{C}_N(t)$ between impulsive instants:

$$\dot{\boldsymbol{C}}_N(t) + \boldsymbol{\mathcal{M}}(t)\boldsymbol{C}_N(t) + \boldsymbol{b}(t) = \mathbf{0}, \;\; \boldsymbol{C}_N(t_{\mathrm{f}}) = \boldsymbol{C}_{\mathrm{f}}, \tag{38}$$

where $\boldsymbol{C}_{\mathrm{f}}$ denote the boundary conditions at the terminal time defined by the user as design parameters, and

$$\begin{aligned}\boldsymbol{\mathcal{M}}(t) &= \langle \boldsymbol{\Phi}_N, \boldsymbol{\Phi}_N\rangle_{\boldsymbol{\Omega}}^{-1} \left\langle \mathbf{J}_{\boldsymbol{x}}(\boldsymbol{\Phi}_N)\boldsymbol{f}_{ct}, \boldsymbol{\Phi}_N\right\rangle_{\boldsymbol{\Omega}} \\ \boldsymbol{b}(t) &= \langle \boldsymbol{\Phi}_N, \boldsymbol{\Phi}_N\rangle_{\boldsymbol{\Omega}}^{-1} \left\langle \boldsymbol{l}_{ct}^{\mathrm{T}}\boldsymbol{l}_{ct}, \boldsymbol{\Phi}_N\right\rangle_{\boldsymbol{\Omega}}.\end{aligned} \tag{39}$$

In summary, the proposed algorithm to compute the storage function in the continuous-time subsystem comprises three steps: $\boldsymbol{f}_{ct}$, $\boldsymbol{l}_{ct}$, $\boldsymbol{\Phi}_N$, and $\boldsymbol{\Omega}$ are first injected into the algorithm as input; three definite n-dimensional integrals, namely $\langle \boldsymbol{\Phi}_N, \boldsymbol{\Phi}_N\rangle$, $\left\langle \mathbf{J}_{\boldsymbol{x}}(\boldsymbol{\Phi}_N)\boldsymbol{f}_{ct}, \boldsymbol{\Phi}_N\right\rangle$, and $\left\langle \boldsymbol{l}_{ct}^{\mathrm{T}}\boldsymbol{l}_{ct}, \boldsymbol{\Phi}_N\right\rangle$, are then computed over the stability region defined by $\boldsymbol{\Omega}$; and a set of ordinary differential equations represented by (38) is ultimately integrated backward in time using a fixed-step numerical scheme, such as the fourth-order Runge–Kutta (RK4) solver,[34] to compute $\boldsymbol{C}_N(t)$ as output.

3.2 | Numerical solution to difference TV-KYP equation

With the continuous-time passivity-based control gain equations thus derived; a set of algebraic equations is developed in this section to approximate the storage function at each impulse. In this regard, the spectral collocation method[34] is utilized to numerically solve the difference TV-KYP equation, (19), at $t = t_k$. The main idea behind the spectral collocation technique is to project the aforementioned equation onto a discrete basis at each impulsive instant to produce as many equations as required for the unknowns. This is analogous to the Galerkin spectral method where the error equation resulting from approximating the storage function is projected onto a truncated set of basis elements to obtain N simultaneous equations for N unknowns.

Preparatory to deriving the discrete-time counterpart of the passivity-based control gain equations, a truncated version of the discretized storage function, (35), is substituted into (19) to formulate the following set of algebraic equations at each jump instant, $t = t_k$:

$$\boldsymbol{\Phi}_N^{\mathrm{T}}(\boldsymbol{x})\Big|_{\boldsymbol{x}=\boldsymbol{f}_{ds}} \boldsymbol{C}_N\left(t_k^+\right) - \boldsymbol{\Phi}_N^{\mathrm{T}}\left(\boldsymbol{x}_k^-\right)\boldsymbol{C}_N\left(t_k^-\right) + \boldsymbol{l}_{ds}^{\mathrm{T}}\left(\boldsymbol{x}_k^-, t_k^-\right)\boldsymbol{l}_{ds}\left(\boldsymbol{x}_k^-, t_k^-\right) = 0. \tag{40}$$

Having $\boldsymbol{C}_N\left(t_k^+\right)$ available from the backward integration of (38), $\boldsymbol{C}_N\left(t_k^-\right)$ can, thus, be computed via the preceding set of equations. However, the state knowledge at $t = t_k^-$, $\boldsymbol{x}_k^-$, is required to reach this objective, which, in consequence, provides a new challenge. Aiming to rise to this challenge, $\boldsymbol{x}_k^-$ is collocated with a suitable set of points, $\bar{\boldsymbol{x}} = \underset{m}{\mathrm{row}}\left\{\bar{\boldsymbol{x}}_m\right\}$ where $\bar{\boldsymbol{x}}_m \in \mathbb{R}^n$ and $m = 1, \ldots, N$, at each impulsive instant to obtain N equations for N unknowns, $\left\{c_j\left(t_k^-\right)\right\}_{j=1}^{N}$. The following set of algebraic equations termed *the discrete-time passivity-based control gain equations* must, therefore, be solved for $\boldsymbol{C}_N\left(t_k^-\right)$ at each impulse:

$$\boldsymbol{C}_N\left(t_k^-\right) = \left(\boldsymbol{\Psi}_k(\bar{\boldsymbol{x}})\right)^{-1}\left[\boldsymbol{\Upsilon}_k\left(\bar{\boldsymbol{x}}, t_k^-\right) + \boldsymbol{\zeta}_k(\bar{\boldsymbol{x}}, t_k^-)\boldsymbol{C}_N\left(t_k^+\right)\right], \tag{41}$$

where

$$\begin{aligned}
\boldsymbol{\Upsilon}_k\left(\bar{\boldsymbol{x}}, t_k^-\right) &= \underset{m}{\text{column}}\left\{\boldsymbol{l}_{ds}^{\mathrm{T}}\left(\bar{\boldsymbol{x}}_m, t_k^-\right)\boldsymbol{l}_{ds}(\bar{\boldsymbol{x}}_m, t_k^-)\right\} \\
&= \begin{bmatrix} \boldsymbol{l}_{ds}^{\mathrm{T}}\left(\bar{\boldsymbol{x}}_1, t_k^-\right)\boldsymbol{l}_{ds}\left(\bar{\boldsymbol{x}}_1, t_k^-\right) \\ \vdots \\ \boldsymbol{l}_{ds}^{\mathrm{T}}\left(\bar{\boldsymbol{x}}_N, t_k^-\right)\boldsymbol{l}_{ds}\left(\bar{\boldsymbol{x}}_N, t_k^-\right) \end{bmatrix}_{N\times 1}, \\
\boldsymbol{\Psi}_k(\bar{\boldsymbol{x}}) &= \underset{m,j}{\text{matrix}}\left\{\phi_j\left(\bar{\boldsymbol{x}}_m\right)\right\} \\
&= \begin{bmatrix} \phi_1\left(\bar{\boldsymbol{x}}_1\right) & \cdots & \phi_N\left(\bar{\boldsymbol{x}}_1\right) \\ \vdots & \ddots & \vdots \\ \phi_1\left(\bar{\boldsymbol{x}}_N\right) & \cdots & \phi_N\left(\bar{\boldsymbol{x}}_N\right) \end{bmatrix}_{N\times N}, \\
\boldsymbol{\zeta}_k\left(\bar{\boldsymbol{x}}, t_k^-\right) &= \underset{m,j}{\text{matrix}}\left\{\left.\phi_j(\boldsymbol{x})\right|_{\boldsymbol{x}=\boldsymbol{f}_{ds}(\bar{\boldsymbol{x}}_m, t_k^-)}\right\} \\
&= \begin{bmatrix} \left.\phi_1(\boldsymbol{x})\right|_{\boldsymbol{x}=\boldsymbol{f}_{ds}(\bar{\boldsymbol{x}}_1, t_k^-)} & \cdots & \left.\phi_N(\boldsymbol{x})\right|_{\boldsymbol{x}=\boldsymbol{f}_{ds}(\bar{\boldsymbol{x}}_1, t_k^-)} \\ \vdots & \ddots & \vdots \\ \left.\phi_1(\boldsymbol{x})\right|_{\boldsymbol{x}=\boldsymbol{f}_{ds}(\bar{\boldsymbol{x}}_N, t_k^-)} & \cdots & \left.\phi_N(\boldsymbol{x})\right|_{\boldsymbol{x}=\boldsymbol{f}_{ds}(\bar{\boldsymbol{x}}_N, t_k^-)} \end{bmatrix}_{N\times N},
\end{aligned} \tag{42}$$

where $\boldsymbol{l}_{ds}\left(\boldsymbol{x}_k^-, t_k^-\right)$ is assumed to serve as a design parameter to be appropriately chosen by the user.

To succinctly summarize, the proposed algorithm for approximating the difference TV-KYP equation, (19), at each impulse is initialized with $\boldsymbol{f}_{ds}$, $\boldsymbol{l}_{ds}$, $\boldsymbol{C}_N\left(t_k^+\right)$, $\boldsymbol{\Phi}_N$, and $\bar{\boldsymbol{x}}$ as input. Constructing arrays of $\boldsymbol{l}_{ds}$ and $\boldsymbol{\Phi}_N$ fed by $\bar{\boldsymbol{x}}$ as shown in (42), an algebraic set of equations given by (41) is then solved at each impulsive instant to compute $\boldsymbol{C}_N\left(t_k^-\right)$ as output.

3.3 | Passivity specifications for hybrid plant

Armed with the continuous-time and discrete-time passivity-based control gain equations, the hybrid nonlinear passivity-based control gain vector can be computed over the entire operating range of the system via solving the following set of equations in an interacting manner for $\boldsymbol{C}_N(t)$:

$$\begin{cases} \dot{\boldsymbol{C}}_N(t) + \boldsymbol{\mathcal{M}}(t)\boldsymbol{C}_N(t) + \boldsymbol{b}(t) = \boldsymbol{0}, \quad \boldsymbol{C}_N\left(t_{\mathrm{f}}\right) = \boldsymbol{C}_{\mathrm{f}} & t \neq t_k \quad \text{See Eq.(39),} \\ \boldsymbol{C}_N\left(t_k^-\right) = \left(\boldsymbol{\Psi}_k(\bar{\boldsymbol{x}})\right)^{-1}\left[\boldsymbol{\Upsilon}_k\left(\bar{\boldsymbol{x}}, t_k^-\right) + \boldsymbol{\zeta}_k(\bar{\boldsymbol{x}}, t_k^-)\boldsymbol{C}_N\left(t_k^+\right)\right] & t = t_k \quad \text{See Eq.(42).} \end{cases} \tag{43}$$

Beginning with the boundary conditions at the terminal time $\boldsymbol{C}_{\mathrm{f}}$, the continuous-time set of equations, which governs the continuous evolution of the passivity-based control gains in the flow manifold, are first integrated backward in time to compute $\boldsymbol{C}_N(t)$ between impulsive instants. Once a specific criterion is met, an impulse is then induced in the solution at $t = t_k$ through applying the discrete-time control gain equations fed by $\boldsymbol{C}_N\left(t_k^+\right)$ and, in consequence, the continuous evolution of $\boldsymbol{C}_N(t)$ is instantaneously switched to a quantum leap occurring in the jump manifold. $\boldsymbol{C}_N\left(t_k^-\right)$ computed at $t = t_k$ is subsequently used as a new set of terminal conditions for the continuous-time control gain equations to be integrated backward in time from t_k^- to t_{k-1}^+. Exhibiting continuous evolution and instantaneous changes on appropriate manifolds, the control gain vector maintains this interacting sequence until the initial time t_0 is reached.

The continuous-time and discrete-time outputs of interest can, now, be determined through (17), (18), (20), and (21). By making use of simplifying assumptions of the form $\boldsymbol{w}_{ct}(\boldsymbol{x}, t) \equiv \boldsymbol{0}$, $\boldsymbol{j}_{ct}(\boldsymbol{x}, t) = \boldsymbol{j}_{ct}^{\mathrm{T}}(\boldsymbol{x}, t)$, $\boldsymbol{w}_{ds}\left(\boldsymbol{x}_k, t_k\right) \equiv \boldsymbol{0}$, and $\boldsymbol{j}_{ds}\left(\boldsymbol{x}_k, t_k\right) = \boldsymbol{j}_{ds}^{\mathrm{T}}\left(\boldsymbol{x}_k, t_k\right)$, which, in fact, limit the design space for each subsystem, the continuous-time and discrete-time outputs of the plant can, thus, be obtained as follows:

$$\begin{aligned} \boldsymbol{h}_{ct}(\boldsymbol{x}, t) &= (1/2)\boldsymbol{g}_{ct}^{\mathrm{T}}(\boldsymbol{x}, t)\mathbf{J}_{\boldsymbol{x}}^{\mathrm{T}}\left(\boldsymbol{\Phi}_N(\boldsymbol{x})\right)\boldsymbol{C}_N(t), \\ \boldsymbol{j}_{ct}(\boldsymbol{x}, t) &= \boldsymbol{0}, \end{aligned} \tag{44}$$

$$\boldsymbol{h}_{ds}\left(\boldsymbol{x}_k, t_k\right) = (1/2)\mathbf{g}_{ds}^{\mathrm{T}}\left(\boldsymbol{x}_k^-, t_k\right)\mathbf{J}_{\boldsymbol{x}}^{\mathrm{T}}\left(\boldsymbol{\Phi}_N(\boldsymbol{x})\right)\Big|_{\boldsymbol{x}=\boldsymbol{f}_{ds}}\boldsymbol{C}_N\left(t_k^+\right),$$

$$\boldsymbol{j}_{ds}\left(\boldsymbol{x}_k, t_k\right) = (1/4)\mathbf{g}_{ds}^{\mathrm{T}}\left(\boldsymbol{x}_k^-, t_k\right)\sum_{j=1}^{N} c_j\left(t_k^+\right)\mathbf{H}_{\boldsymbol{x}}\left(\phi_j(\boldsymbol{x})\right)\Big|_{\boldsymbol{x}=\boldsymbol{f}_{ds}}\boldsymbol{g}_{ds}\left(\boldsymbol{x}_k^-, t_k\right), \tag{45}$$

where $\mathbf{H}_{\boldsymbol{x}}$ denotes the Hessian matrix with respect to $\boldsymbol{x}$.

With the hybrid output of interest thus determined, a hybrid controller capable of meeting the input strict passivity requirements remains to be designed to construct closed-loop stability. With this aim in view, two distinct structures are employed in the following subsections to synthesize the hybrid nonlinear controller in question: a static compensator, which serves to provide proportional output feedback with constant positive gains in each continuous-time and discrete-time subsystem; and a dynamic compensator, the state of which evolves both continuously and discontinuously on appropriate manifolds as time elapses. In both architectures, external disturbances acting on the closed-loop system are assumed to be sufficiently small, that is, $(\boldsymbol{d}_{ct}, \boldsymbol{d}_{ds}) \cong (\mathbf{0}, \mathbf{0})$, and, in consequence, the hybrid output of the controller, $\left(\widehat{\boldsymbol{y}}_{ct}, \widehat{\boldsymbol{y}}_{ds}\right)$, is directly fed back to the plant with negative sign as its hybrid input (See Figure 1). It is noteworthy that the plant dynamics are also presupposed to evolve periodically over time for the purpose of synthesizing hybrid nonlinear time-varying controllers with enhanced global performance.[1] Therefore, asymptotic stability properties are no longer restricted to the time interval from 0 to t_{f}, and can be repeated over the entire operating range of the system.

3.4 | Closed-loop stability: static compensator

With the purpose of constructing a stable closed-loop system, a static controller in the form of a hybrid proportional output feedback compensator with constant positive gains, that is, $\boldsymbol{\mathcal{H}} \triangleq (\boldsymbol{K}_{ct}, \boldsymbol{K}_{ds})$ where $\boldsymbol{K}_{ct} = \boldsymbol{K}_{ct}^{\mathrm{T}} > \mathbf{0}$ and $\boldsymbol{K}_{ds} = \boldsymbol{K}_{ds}^{\mathrm{T}} > \mathbf{0}$, is employed in this section to meet the input strict passivity requirements. As the proposed static compensator benefits inherently from the input strict passivity properties, provided that $(\boldsymbol{K}_{ct}, \boldsymbol{K}_{ds}) > (\mathbf{0}, \mathbf{0})$, there is no necessity to use the corresponding strict passivity-related TV-KYP conditions, and the closed-loop stability can simply be established by interconnecting the plant dynamics, which are now guaranteed to be passive, and the static controller through negative feedback. In this regard, the eigendecomposition of proportional gain matrix can be used to demonstrate the input strict passivity of the static compensator. Since $\left(\boldsymbol{u}_{ct}, \boldsymbol{u}_{ds,k}\right) = -\left(\widehat{\boldsymbol{y}}_{ct}, \widehat{\boldsymbol{y}}_{ds}\right) = -\left(\boldsymbol{K}_{ct}\widehat{\boldsymbol{u}}_{ct}, \boldsymbol{K}_{ds}\widehat{\boldsymbol{u}}_{ds,k}\right) = -\left(\boldsymbol{K}_{ct}\boldsymbol{y}_{ct}, \boldsymbol{K}_{ds}\boldsymbol{y}_{ds}\right)$, the desired hybrid nonlinear passivity-based control law can, thus, be formulated as follows:

$$\begin{cases} \boldsymbol{u}_{ct}(\boldsymbol{x}, t) = -\boldsymbol{K}_{ct}\boldsymbol{h}_{ct} & t \neq t_k \\ \boldsymbol{u}_{ds,k} = -\left(\mathbf{1}_{m_{ds}\times m_{ds}} + \boldsymbol{K}_{ds}\boldsymbol{j}_{ds}\right)^{-1}\boldsymbol{K}_{ds}\boldsymbol{h}_{ds} & t = t_k \end{cases}. \tag{46}$$

3.5 | Closed-loop stability: Dynamic compensator

Aiming to enhance the control authority and to filter out sensor noise, which, in turn, contributes significantly to the first objective, a compensator of a dynamic nature is adopted in this section to be interconnected with the passive plant through negative feedback. The idea of using a dynamic compensator in a feedback path has origins in Reference 35 where, in compliance with the positive real design procedure, the continuous-time linear time-invariant (LTI) KYP conditions were used to develop an embedded control architecture involving a strictly positive real (continuous-time) LTI dynamic compensator in order to stabilize large-scale space structures. Complementing the aforementioned continuous-time dynamics with discrete-time events occurring at an appropriate sequence of time instants, together with endowing the resultant dynamics with a time-dependent character, this article proposes a time-varying control-affine structure involving an interacting pair of continuous-time and discrete-time dynamics to serve as the dynamic compensator in question as follows:

$$\boldsymbol{\mathcal{H}} \triangleq \begin{cases} \begin{cases} \dot{\widehat{\boldsymbol{x}}}(t) = \widehat{\boldsymbol{A}}_{ct}(t)\widehat{\boldsymbol{x}} + \widehat{\boldsymbol{B}}_{ct}(t)\widehat{\boldsymbol{u}}_{ct}(t), \widehat{\boldsymbol{x}}(t_0) = \widehat{\boldsymbol{x}}_0 & (47) \\ \widehat{\boldsymbol{y}}_{ct}(t) = \widehat{\boldsymbol{C}}_{ct}(t)\widehat{\boldsymbol{x}} + \widehat{\boldsymbol{D}}_{ct}(t)\widehat{\boldsymbol{u}}_{ct}(t) & (48) \end{cases} & t \neq t_k \\ \begin{cases} \widehat{\boldsymbol{x}}_k^+ = \widehat{\boldsymbol{A}}_{ds}(t)\widehat{\boldsymbol{x}}_k^- + \widehat{\boldsymbol{B}}_{ds}(t)\widehat{\boldsymbol{u}}_{ds,k} & (49) \\ \widehat{\boldsymbol{y}}_{ds}(t) = \widehat{\boldsymbol{C}}_{ds}(t)\widehat{\boldsymbol{x}}_k^- + \widehat{\boldsymbol{D}}_{ds}(t)\widehat{\boldsymbol{u}}_{ds,k} & (50) \end{cases} & t = t_k \end{cases},$$

where $\widehat{\boldsymbol{x}}$ is the (virtual) state of the controller and $\widehat{\boldsymbol{x}}_k^{\pm} \triangleq \widehat{\boldsymbol{x}}\left(t_k^{\pm}\right)$ represent the controller's state vector immediately before and after impulsive actions at $t = t_k$. Furthermore, $\widehat{\boldsymbol{A}}_{ct}$, $\widehat{\boldsymbol{B}}_{ct}$, $\widehat{\boldsymbol{C}}_{ct}$, $\widehat{\boldsymbol{D}}_{ct}$, $\widehat{\boldsymbol{A}}_{ds}$, $\widehat{\boldsymbol{B}}_{ds}$, $\widehat{\boldsymbol{C}}_{ds}$, and $\widehat{\boldsymbol{D}}_{ds}$ denote the time-dependent system matrices, with appropriate dimensions, associated with the continuous-time and discrete-time subsystems of $\boldsymbol{\mathcal{H}}$. With (48) and (50) in mind, since $\left(\widehat{\boldsymbol{u}}_{ct}, \widehat{\boldsymbol{u}}_{ds,k}\right) = \left(\boldsymbol{y}_{ct}, \boldsymbol{y}_{ds}\right)$ and $\left(\widehat{\boldsymbol{y}}_{ct}, \widehat{\boldsymbol{y}}_{ds}\right) = -\left(\boldsymbol{u}_{ct}, \boldsymbol{u}_{ds,k}\right)$, the hybrid passivity-based control input to be determined can be formulated in the following form:

$$\begin{cases} \boldsymbol{u}_{ct}(\boldsymbol{x}, \widehat{\boldsymbol{x}}, t) = -\widehat{\boldsymbol{C}}_{ct}(t)\widehat{\boldsymbol{x}} - \widehat{\boldsymbol{D}}_{ct}(t)\boldsymbol{y}_{ct} & t \neq t_k, \\ \boldsymbol{u}_{ds}\left(\boldsymbol{x}_k^-, \widehat{\boldsymbol{x}}_k^-, t_k\right) = -\widehat{\boldsymbol{C}}_{ds}(t)\widehat{\boldsymbol{x}}_k^- - \widehat{\boldsymbol{D}}_{ds}(t)\boldsymbol{y}_{ds} & t = t_k. \end{cases} \tag{51}$$

With the hybrid output dynamics of interest thus computed, the main challenge is now to determine the time-dependent matrices present in (47)–(50) such that the input strict passivity requirements are met for $\boldsymbol{\mathcal{H}}$. With this aim in view, the strict passivity-related TV-KYP conditions given by (28)–(33) with $\varepsilon_{ct} > 0$ and $\varepsilon_{ds} > 0$ (corresponding to the structure of (47)–(50) which are linear in $\widehat{\boldsymbol{x}}$) are first fed with the $\boldsymbol{\mathcal{H}}$-related system matrices and then employed to characterize input strict passivity for $\boldsymbol{\mathcal{H}}$. By considering $\boldsymbol{L}_{ct}$, $\boldsymbol{W}_{ct}$, ε_{ct}, $\boldsymbol{L}_{ds}$, $\boldsymbol{W}_{ds}$, and ε_{ds} as design parameters to be appropriately selected by the user, the outcome is, nevertheless, an underdetermined set of equations (i.e., the resultant six equations involve 10 unknowns), which, in turn, presents a new challenge. Aiming to rise to these challenges, the following three-step design procedure is proposed in this article. In the first step, $\widehat{\boldsymbol{C}}_{ct}$, $\widehat{\boldsymbol{C}}_{ds}$, $\widehat{\boldsymbol{A}}_{ct}$, and $\widehat{\boldsymbol{A}}_{ds}$ are selected in a judicious manner to render (28)–(33) determined, while simultaneously guaranteeing asymptotic stability for $\boldsymbol{\mathcal{H}}$; the resultant differential and difference TV-KYP equations, (28) and (31) respectively, are then solved for $\boldsymbol{P}(t)$ in an interacting manner; and $\widehat{\boldsymbol{B}}_{ct}$, $\widehat{\boldsymbol{D}}_{ct}$, $\widehat{\boldsymbol{B}}_{ds}$, and $\widehat{\boldsymbol{D}}_{ds}$ are ultimately computed via the remaining TV-KYP equations (where $\varepsilon_{ct} > 0$ and $\varepsilon_{ds} > 0$).

Instead of arbitrarily assigning $\widehat{\boldsymbol{C}}_{ct}$, $\widehat{\boldsymbol{C}}_{ds}$, $\widehat{\boldsymbol{A}}_{ct}$, and $\widehat{\boldsymbol{A}}_{ds}$, this article proposes the hybrid linear quadratic regulator (LQR) policy (See Reference 36 for a concise form of the hybrid LQR formulation), amongst all possible approaches, to accomplish the first objective. In this regard, a hybrid LQR formulation with finite-time horizon, which simultaneously combines the continuous-time set of differential Riccati equations with discrete-time Riccati events, is first set up as per the linearized equations of the plant dynamics given by (24)–(27) in an attempt to render the (underdetermined) equations (28)–(33) with $\varepsilon_{ct} > 0$ and $\varepsilon_{ds} > 0$ determined, while simultaneously ensuring that the dynamics of $\boldsymbol{\mathcal{H}}$ are asymptotically stable. Once the time-varying Riccati solutions are computed over the entire operating time, the resultant continuous-time and discrete-time optimal gain matrices are then assigned to $\widehat{\boldsymbol{C}}_{ct}$ and $\widehat{\boldsymbol{C}}_{ds}$, respectively. Given a hybrid quadratic performance index of the form:

$$\mathcal{J} = \int_{t_0}^{t_f} \left(\boldsymbol{x}^{\mathrm{T}}(t)\boldsymbol{Q}_{ct}\boldsymbol{x}(t) + \boldsymbol{u}_{ct}^{\mathrm{T}}(t)\boldsymbol{R}_{ct}\boldsymbol{u}_{ct}(t)\right) \mathrm{d}t + \sum_{k=1}^{\mathcal{K}} \left(\boldsymbol{x}_k^{-\mathrm{T}}\boldsymbol{Q}_{ds}\boldsymbol{x}_k^- + \boldsymbol{u}_{ds,k}^{\mathrm{T}}\boldsymbol{R}_{ds}\boldsymbol{u}_{ds,k}\right), \tag{52}$$

where $\mathcal{K}$ specifies the total number of impulses applied during the operating period, and $\boldsymbol{Q}_{ct} = \boldsymbol{Q}_{ct}^{\mathrm{T}} \in \mathbb{R}^{n\times n} \geq \boldsymbol{0}$, $\boldsymbol{R}_{ct} = \boldsymbol{R}_{ct}^{\mathrm{T}} \in \mathbb{R}^{m_{ct}\times m_{ct}} > \boldsymbol{0}$, $\boldsymbol{Q}_{ds} = \boldsymbol{Q}_{ds}^{\mathrm{T}} \in \mathbb{R}^{n\times n} \geq \boldsymbol{0}$, and $\boldsymbol{R}_{ds} = \boldsymbol{R}_{ds}^{\mathrm{T}} \in \mathbb{R}^{m_{ds}\times m_{ds}} > \boldsymbol{0}$ denote the continuous-time and discrete-time weighting matrices acting on the state and control; it is well known that the hybrid Riccati-based control law, which minimizes the hybrid performance index represented by (52), can be obtained by the following pair of optimal control inputs:

$$\begin{cases} \boldsymbol{v}_{ct}^*(\boldsymbol{x}, t) &= -\boldsymbol{R}_{ct}^{-1}\boldsymbol{B}_{ct}^{\mathrm{T}}\boldsymbol{\Gamma}(t)\boldsymbol{x}(t) & t \neq t_k, \\ \boldsymbol{v}_{ds,k}^*(\boldsymbol{x}_k, t_k) &= -\boldsymbol{R}_{ds}^{-1}\boldsymbol{B}_{ds}^{\mathrm{T}}\boldsymbol{A}_{ds}^{-\mathrm{T}}\left[\boldsymbol{\Gamma}_k^- - \boldsymbol{Q}_{ds}\right]\boldsymbol{x}_k^- & t = t_k, \end{cases} \tag{53}$$

where $\boldsymbol{\Gamma}(t) = \boldsymbol{\Gamma}^{\mathrm{T}}(t) \geq \boldsymbol{0}$ represent the time-varying Riccati solutions. In this regard, $\boldsymbol{\Gamma}(t)$ can be computed via integrating the following continuous-time set of differential Riccati equations backward in time from $t = t_f$ to $t = t_0$, given the boundary conditions at the terminal time $\boldsymbol{\Gamma}(t_f) = \boldsymbol{0}$, under the influence of jumps inducing in the matrix solution via provoking the discrete-time set of Riccati equations at $t = t_k$:

$$\begin{cases} \dot{\boldsymbol{\Gamma}}(t) + \boldsymbol{A}_{ct}^{\mathrm{T}}\boldsymbol{\Gamma}(t) + \boldsymbol{\Gamma}(t)\boldsymbol{A}_{ct} + \boldsymbol{Q}_{ct} - \boldsymbol{\Gamma}(t)\boldsymbol{B}_{ct}\boldsymbol{R}_{ct}^{-1}\boldsymbol{B}_{ct}^{\mathrm{T}}\boldsymbol{\Gamma}(t) = \boldsymbol{0}, \ \boldsymbol{\Gamma}(t_f) = \boldsymbol{0}, & t \neq t_k, \\ \boldsymbol{\Gamma}_k^- = \boldsymbol{Q}_{ds} + \boldsymbol{A}_{ds}^{\mathrm{T}}\boldsymbol{\Gamma}_k^+\boldsymbol{A}_{ds} - \boldsymbol{A}_{ds}^{\mathrm{T}}\boldsymbol{\Gamma}_k^+\boldsymbol{B}_{ds}\left[\boldsymbol{R}_{ds} + \boldsymbol{B}_{ds}^{\mathrm{T}}\boldsymbol{\Gamma}_k^+\boldsymbol{B}_{ds}\right]^{-1}\boldsymbol{B}_{ds}^{\mathrm{T}}\boldsymbol{\Gamma}_k^+\boldsymbol{A}_{ds}, & t = t_k. \end{cases} \tag{54}$$

With (51) and (53) in mind, $\widehat{\boldsymbol{C}}_{ct}$ and $\widehat{\boldsymbol{C}}_{ds}$ are therefore determined as follows:

$$\widehat{\boldsymbol{C}}_{ct}(t) = \boldsymbol{R}_{ct}^{-1}\boldsymbol{B}_{ct}^{\mathrm{T}}\boldsymbol{\Gamma}(t), \tag{55}$$

$$\widehat{\boldsymbol{C}}_{ds}(t_k) = \boldsymbol{R}_{ds}^{-1}\boldsymbol{B}_{ds}^{\mathrm{T}}\boldsymbol{A}_{ds}^{-\mathrm{T}}\left[\boldsymbol{\Gamma}_k^- - \boldsymbol{Q}_{ds}\right]. \tag{56}$$

Proceeding with the above-mentioned hybrid LQR formulation further, $\widehat{\boldsymbol{A}}_{ct}$ and $\widehat{\boldsymbol{A}}_{ds}$ are then selected such that the hybrid dynamic compensator represented by (47)–(50) is guaranteed to be asymptotically stable, that is,

$$\begin{aligned}\widehat{\boldsymbol{A}}_{ct}(t) &= \boldsymbol{A}_{ct} - \boldsymbol{B}_{ct}\widehat{\boldsymbol{C}}_{ct}\\ &= \boldsymbol{A}_{ct} - \boldsymbol{B}_{ct}\boldsymbol{R}_{ct}^{-1}\boldsymbol{B}_{ct}^{\mathrm{T}}\boldsymbol{\Gamma}(t),\end{aligned} \tag{57}$$

$$\begin{aligned}\widehat{\boldsymbol{A}}_{ds}(t_k) &= \boldsymbol{A}_{ds} - \boldsymbol{B}_{ds}\widehat{\boldsymbol{C}}_{ds}\\ &= \boldsymbol{A}_{ds} - \boldsymbol{B}_{ds}\boldsymbol{R}_{ds}^{-1}\boldsymbol{B}_{ds}^{\mathrm{T}}\boldsymbol{A}_{ds}^{-\mathrm{T}}\left[\boldsymbol{\Gamma}_k^- - \boldsymbol{Q}_{ds}\right],\end{aligned} \tag{58}$$

where $(\boldsymbol{A}_{ct}, \boldsymbol{B}_{ct})$ and $(\boldsymbol{A}_{ds}, \boldsymbol{B}_{ds})$ are assumed to be controllable.

Proceeding to the second step, the linear strict passivity-based gain matrix, $\boldsymbol{P}(t)$, can be computed, with $\widehat{\boldsymbol{A}}_{ct}$ and $\widehat{\boldsymbol{A}}_{ds}$ thus determined, through solving (28) and (31) simultaneously in an interacting manner as follows:

$$\begin{cases}\dot{\boldsymbol{P}}(t) + \widehat{\boldsymbol{A}}_{ct}^{\mathrm{T}}\boldsymbol{P}(t) + \boldsymbol{P}(t)\widehat{\boldsymbol{A}}_{ct} + \boldsymbol{L}_{ct}^{\mathrm{T}}\boldsymbol{L}_{ct} = \boldsymbol{0}, \ \boldsymbol{P}(t_{\mathrm{f}}) = \boldsymbol{P}_{\mathrm{f}}, & t \neq t_k,\\ \boldsymbol{P}_k^- = \widehat{\boldsymbol{A}}_{ds}^{\mathrm{T}}\boldsymbol{P}_k^+\widehat{\boldsymbol{A}}_{ds} + \boldsymbol{L}_{ds}^{\mathrm{T}}\boldsymbol{L}_{ds}, & t = t_k,\end{cases} \tag{59}$$

where $\boldsymbol{P}_k^{\pm} \triangleq \boldsymbol{P}\left(t_k^{\pm}\right)$ and $\boldsymbol{P}_{\mathrm{f}} = \boldsymbol{P}_{\mathrm{f}}^{\mathrm{T}} \geq \boldsymbol{0}$ specify the boundary conditions at the terminal time defined by the user as design parameters.

In the final step, simplifying assumptions in the form of $\boldsymbol{W}_{ct} \equiv \boldsymbol{0}$, $\widehat{\boldsymbol{D}}_{ct} = \widehat{\boldsymbol{D}}_{ct}^{\mathrm{T}}$, $\boldsymbol{W}_{ds} \equiv \boldsymbol{0}$, and $\widehat{\boldsymbol{D}}_{ds} = \widehat{\boldsymbol{D}}_{ds}^{\mathrm{T}}$ are made to limit the design space in each continuous-time and discrete-time subsystem; and $\widehat{\boldsymbol{B}}_{ct}$, $\widehat{\boldsymbol{D}}_{ct}$, $\widehat{\boldsymbol{B}}_{ds}$, and $\widehat{\boldsymbol{D}}_{ds}$ are ultimately computed, respectively, via (29), (30), (32), and (33) as follows:

$$\widehat{\boldsymbol{B}}_{ct}(t) = \boldsymbol{P}^{-1}(t)\widehat{\boldsymbol{C}}_{ct}^{\mathrm{T}}, \tag{60}$$

$$\widehat{\boldsymbol{D}}_{ct}(t) = \widehat{\boldsymbol{D}}_{ct} = \varepsilon_{ct}\boldsymbol{1}_{m_{ct}\times m_{ct}}, \tag{61}$$

$$\widehat{\boldsymbol{B}}_{ds}(t_k) = \left(\widehat{\boldsymbol{A}}_{ds}^{\mathrm{T}}\boldsymbol{P}_k^+\right)^{-1}\widehat{\boldsymbol{C}}_{ds}^{\mathrm{T}}, \tag{62}$$

$$\widehat{\boldsymbol{D}}_{ds}(t_k) = \varepsilon_{ds}\boldsymbol{1}_{m_{ds}\times m_{ds}} + (1/2)\widehat{\boldsymbol{B}}_{ds}^{\mathrm{T}}\boldsymbol{P}_k^+\widehat{\boldsymbol{B}}_{ds}. \tag{63}$$

As is apparent from equation (60), the controllability of the pair $\left(\widehat{\boldsymbol{A}}_{ct}, \widehat{\boldsymbol{B}}_{ct}\right)$ along with the observability of the pairs $\left(\widehat{\boldsymbol{C}}_{ct}, \widehat{\boldsymbol{A}}_{ct}\right)$ and $\left(\boldsymbol{L}_{ct}, \widehat{\boldsymbol{A}}_{ct}\right)$ are additionally required to render $\boldsymbol{P}(t)$ invertible in order to compute $\widehat{\boldsymbol{B}}_{ct}$.

All the required ingredients are now in place to find the desired hybrid nonlinear passivity-based control law. To this end, $\widehat{\boldsymbol{C}}_{ct}$, $\widehat{\boldsymbol{C}}_{ds}$, $\widehat{\boldsymbol{D}}_{ct}$, and $\widehat{\boldsymbol{D}}_{ds}$ (computed from (55), (56), (61), and (63), respectively) along with the hybrid output of the plant represented by (44) and (45) are therefore substituted into (51) to obtain the following hybrid pair of passivity-based control inputs:

$$\begin{cases}\boldsymbol{u}_{ct}(\boldsymbol{x}, \widehat{\boldsymbol{x}}, t) = -\widehat{\boldsymbol{C}}_{ct}\widehat{\boldsymbol{x}}(t) - \widehat{\boldsymbol{D}}_{ct}\boldsymbol{h}_{ct}, & t \neq t_k,\\ \boldsymbol{u}_{ds}\left(\boldsymbol{x}_k^-, \widehat{\boldsymbol{x}}_k^-, t_k^+\right) = -\left(\boldsymbol{1}_{m_{ds}\times m_{ds}} + \widehat{\boldsymbol{D}}_{ds}\boldsymbol{j}_{ds}\right)^{-1}\left(\widehat{\boldsymbol{C}}_{ds}\widehat{\boldsymbol{x}}_k^- + \widehat{\boldsymbol{D}}_{ds}\boldsymbol{h}_{ds}\right), & t = t_k.\end{cases} \tag{64}$$

Figure 2 succinctly summarizes the proposed three-step control design algorithm pursued in the preceding sections to derive the desired hybrid nonlinear passivity-based control architectures. Aiming to determine the hybrid output dynamics of the plant which satisfy the passivity properties from input to output, given the heterogeneous dynamics of the system, a discretized representation of the storage function involving a prescribed state-dependent set of basis functions $\boldsymbol{\Phi}_N(\boldsymbol{x}) = [\phi_1(\boldsymbol{x}) \ \ldots \ \phi_N(\boldsymbol{x})]^{\mathrm{T}}$ and their entangled time-dependent coefficients (termed *the hybrid nonlinear passivity-based control gains*) $\boldsymbol{C}_N(t) = [c_1(t) \ \ldots \ c_N(t)]^{\mathrm{T}}$ is first substituted into the differential and difference TV-KYP

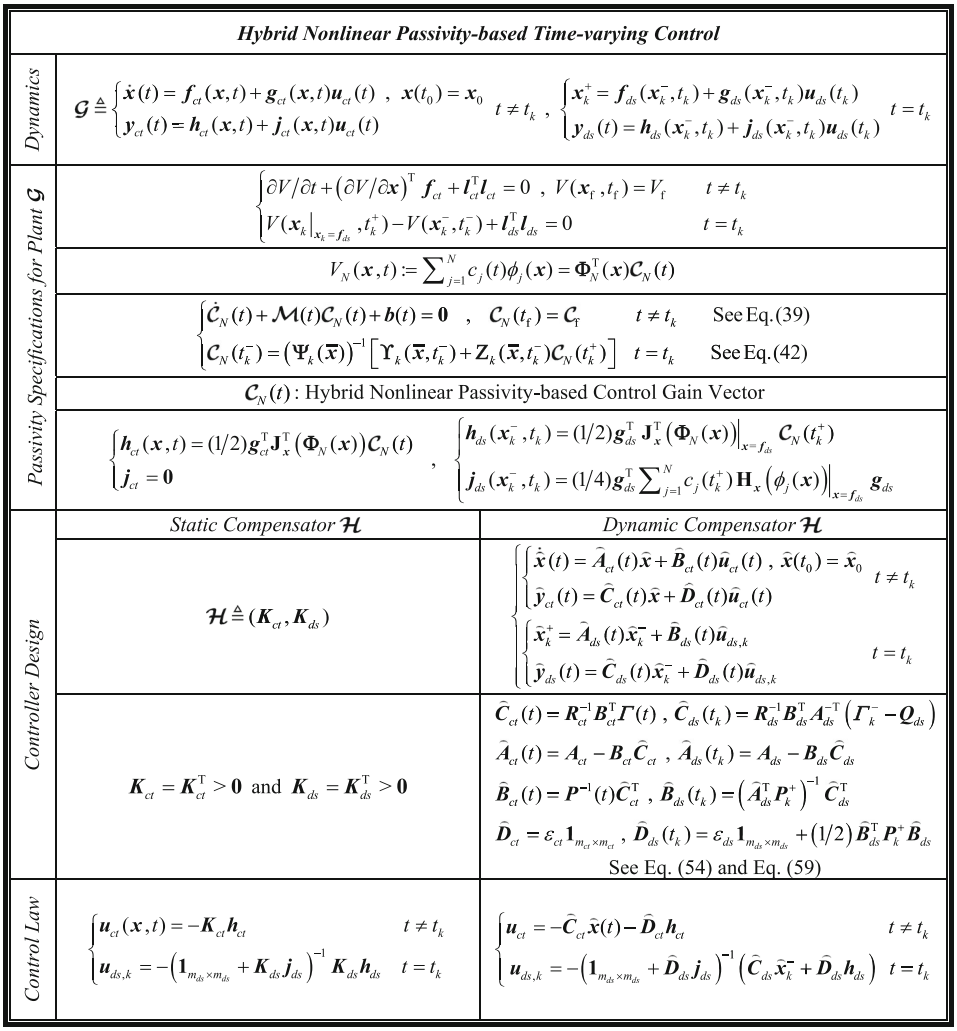

FIGURE 2 Hybrid nonlinear passivity-based control using static and dynamic compensators.

equations represented by (16) and (19). The resultant hybrid set of equations described by (43) is then solved in an interacting manner for $\boldsymbol{\mathcal{C}}_N(t)$ in both continuous-time and discrete-time subsystems. The first step, therefore, ends by injecting the computed passivity-based control gains into (44) and (45) to obtain the hybrid output dynamics of interest. Proceeding to the second step, hybrid compensators of static and dynamic structures are separately designed to meet the input strict passivity requirements. Whereas the static compensator benefits inherently from the input strict passivity properties, provided that $(\boldsymbol{K}_{ct}, \boldsymbol{K}_{ds}) > (\boldsymbol{0}, \boldsymbol{0})$, the time-dependent system matrices involved in the structure of the dynamic compensator in question are determined by simultaneous utilization of the hybrid finite-time horizon LQR scheme formulated by (52)–(54) and the strict passivity-related TV-KYP conditions represented by (28)–(33) with $\varepsilon_{ct} > 0$ and $\varepsilon_{ds} > 0$. In the last step, the resultant plant dynamics and controller are interconnected through negative feedback to establish the closed-loop stability in accordance with the passivity theorem.

4 | PRACTICAL CONSIDERATIONS

Given the heterogeneous dynamics of the plant to be controlled in nonlinear forms, three major parameters must be selected appropriately to apply the hybrid numerical algorithm developed in Section 3.3: a compact set which contains the origin as an interior point and is preferably symmetric about it, a set of basis functions which can adequately approximate the storage function involved in the differential and difference TV-KYP equations, and a set of collocation points which are located inside and on the boundaries of the compact set.

The compact set (or stability region or a bounded domain of the state space), $\boldsymbol{\Omega}$, is defined as the domain of possible values for the states. $\boldsymbol{\Omega}$ can be determined according to kinematical or practical limitations of the system, together with

the likely deviation of the system states from their nominal value of zero. For instance, when an attitude control problem using modified Rodrigues parameters is concerned, the stability region associated with the attitude parameters must be restricted to $(-2\pi, 2\pi)$ in order to ovoid their singularities occurring at -2π and 2π. For angular velocity components, however, there are no kinematical limitations; their domain of possible values can, therefore, be selected on the basis of practical considerations.

Proper selection of basis functions is critical to synthesize the nonlinear passivity-based controllers in question. Two important requirements pertaining to the structure and number of basis elements, namely, *characteristic* and *quantity requirements*, must be satisfied in order to make an appropriate choice of basis functions. The main objective being pursued by the characteristic requirement is to synthesize a controller by which the essential nonlinear terms involved in the dynamics of the system are spanned by the basis functions, and hence effectively captured. Basis elements are therefore configured such that the constituent linear and nonlinear terms of the system dynamics are incorporated into the control law. The resultant controller therefore wields authority to compensate adequately for the nonlinear dynamics of the system. Furthermore, the number of basis elements must be sufficiently large to approximate the storage function with sufficient accuracy (*quantity requirement*). The accuracy of $V_N(\boldsymbol{x}, t)$ is therefore predicated upon both characteristics and quantities of the basis elements selected to form the approximation. In addition to the characteristic and quantity requirements stressed in the preceding, an appropriate choice of basis functions must also produce an invertible $\langle \boldsymbol{\Phi}_N, \boldsymbol{\Phi}_N \rangle_{\boldsymbol{\Omega}}$ to render (39) solvable.

As demonstrated in the literature, polynomials have been proven to serve effectively as basis functions in algorithms where the Galerkin-based projection is used to approximate the steady-state version of the Hamilton-Jacobi-Bellman[37] and Hamilton-Jacobi-Isaac[38] equations. To the knowledge of the authors, the best way to find appropriate selection of basis functions for time-dependent dynamical systems is to commence with the quadratic basis elements obtained by the second-order expansion of the system state, eliminating those terms whose corresponding control gains are either zero or very small as compared to the other terms. The remaining quadratic basis elements must, then, be augmented by further higher-order terms to capture the essential nonlinear dynamics of the system. Due to multiplication of $\boldsymbol{g}_{ct}^{\mathrm{T}}(\boldsymbol{x}, t)$ and $\boldsymbol{g}_{ds}^{\mathrm{T}}(\boldsymbol{x}_k, t_k)$ with $\mathbf{J}_{\boldsymbol{x}}^{\mathrm{T}}(\boldsymbol{\Phi}_N(\boldsymbol{x}))$ in the configuration of the proposed passivity-based control laws given by (46) and (51); these additional higher-order basis elements must be selected such that their partial derivatives with respect to *gain-effective states* (those states which correspond to nonzero elements of $\boldsymbol{g}_{ct}^{\mathrm{T}}$ and $\boldsymbol{g}_{ds}^{\mathrm{T}}$, thereby contributing substantially to preserve non-zero control gains) result in functions of the states desired to ultimately appear in the passivity-based control laws to capture the dominant nonlinear dynamics of the system. For clarification, consider a four-dimensional continuous-time system with the following control input function:

$$\boldsymbol{g}_{ct}(\boldsymbol{x}, t) = \begin{bmatrix} 0 & 0 & g_{31} & 0 \\ 0 & 0 & 0 & g_{42} \end{bmatrix}^{\mathrm{T}},$$

where $\boldsymbol{x} = [x_1 \;\; x_2 \;\; x_3 \;\; x_4]^{\mathrm{T}}$, and g_{31} and g_{42} represent the non-zero elements of $\boldsymbol{g}_{ct}$. Since x_3 and x_4 (associated with g_{31} and g_{42}, respectively) act as the gain-effective states for the problem in hand, any basis element consisting of either x_3 and x_4 will show up in the passivity-based control law as demonstrated below:

$$\begin{aligned} \boldsymbol{u}_{ct}(\boldsymbol{x}, t) &= -\frac{1}{2}\boldsymbol{K}_{ct}\boldsymbol{g}_{ct}^{\mathrm{T}}\mathbf{J}_{\boldsymbol{x}}^{\mathrm{T}}(\boldsymbol{\Phi}_N(\boldsymbol{x}))\,\boldsymbol{C}_N(t) \\ &= -\frac{1}{2}\boldsymbol{K}_{ct}\begin{bmatrix} 0 & 0 & g_{31} & 0 \\ 0 & 0 & 0 & g_{42} \end{bmatrix}\begin{bmatrix} \frac{\partial \phi_1}{\partial x_1} & \cdots & \frac{\partial \phi_N}{\partial x_1} \\ \vdots & \ddots & \vdots \\ \frac{\partial \phi_1}{\partial x_4} & \cdots & \frac{\partial \phi_N}{\partial x_4} \end{bmatrix}\begin{bmatrix} c_1(t) \\ \vdots \\ c_N(t) \end{bmatrix} \\ &= -\frac{1}{2}\boldsymbol{K}_{ct}\begin{bmatrix} g_{31}\frac{\partial \phi_1}{\partial x_3} & \cdots & g_{31}\frac{\partial \phi_N}{\partial x_3} \\ g_{42}\frac{\partial \phi_1}{\partial x_4} & \cdots & g_{42}\frac{\partial \phi_N}{\partial x_4} \end{bmatrix}\begin{bmatrix} c_1(t) \\ \vdots \\ c_N(t) \end{bmatrix}. \end{aligned}$$

Additional higher-order basis elements must, therefore, be selected such that their partial derivatives with respect to x_3 and x_4 give rise to functions of $\boldsymbol{x}$ intended to ultimately emerge in the control law, and hence capture the significant nonlinear dynamics of the system. For example, if the system being considered possesses dynamics involving a nonlinear term such as $x_1^2 x_2$, basis elements of the form $x_1^2 x_2 x_3$ or $x_1^2 x_2 x_4$ (or even $x_1^2 x_2 x_3 x_4$) will eventually produce $x_1^2 x_2$ in the passivity-based control law to capture the foregoing nonlinear term.

By increasing the number of basis elements in a manner consistent with the characteristic requirements, $V_N(\boldsymbol{x}, t)$gradually approaches $V(\boldsymbol{x}, t)$. At a certain number of basis elements, satisfactory performance is ultimately obtained and, in consequence, the quantity requirement is fulfilled, that is, $V_N \cong V$. Henceforth, any further increase in the number of basis elements yields insignificant improvement in the system performance at the expense of computational cost.

Due to entanglement between prescribed state-dependent basis functions, $\left\{\phi_j(\boldsymbol{x})\right\}_{j=1}^{N}$, and time-dependent coefficients, $\left\{c_j(t)\right\}_{j=1}^{N}$, in forming a discretized representation of $V(\boldsymbol{x}, t)$, each $c_j(t)$ corresponds intimately to a specific basis element $\phi_j(\boldsymbol{x})$, and, in turn, evolves in accordance with the character of this very basis element in addition to the dynamics of the system. As a consequence, since basis functions are selected in compliance with the system dynamics, time-dependent control gains duplicate the dynamical behavior of the system. For example, for a controllable system whose dynamics enjoy periodic properties, $\left\{c_j(t)\right\}_{j=1}^{N}$ evolve periodically in the steady-state phase.

A suitable set of collocation points is also necessary to design the discrete-time portion of the hybrid nonlinear passivity-based controller. Collocation points can be selected from the entire compact set excluding the origin, provided that the rank condition required to render $\boldsymbol{\Psi}_k(\bar{\boldsymbol{x}})$ invertible is satisfied for solving (41).

All computations involved in the proposed hybrid control algorithms are performed off-line (prior to implementation); once the passivity-based control gains, $\boldsymbol{C}_N(t)$, are computed through solving (43) in an interacting manner, the derived control architectures can be implemented in hardware and run in real time. Moreover, there are possibilities to facilitate the implementation process of the proposed control schemes. For instance, assuming a periodic or quasi-periodic character for the time-varying passivity-based control gains over the operating time, Fourier series[39] can be employed to approximate the steady-state portion of $\boldsymbol{C}_N(t)$ by discarding the initial transient phase coming backward from t_f. Rather than storing the entire time history of $\boldsymbol{C}_N(t)$, the Fourier-based approximate coefficients can be stored on-board. As a direct consequence, not only is the storage memory requirement significantly reduced, but also $\boldsymbol{C}_N(t)$ computed by a backward integration process prior to implementation are also no longer restricted to the time interval from 0 to t_f (defined by the user during control design) and can, in turn, be extended globally to any desired operating time of an arbitrary length. However, the number of coefficients present in Fourier series must be sufficiently large to accurately capture the actual periodic part of $\boldsymbol{C}_N(t)$.

Lastly, since the discrete-time passivity-based control gain equations, (41), and the discrete-time dynamics, (3), require, respectively, the knowledge of the time-varying control gains at $t = t_k^+$ (i.e., $\boldsymbol{C}_N\left(t_k^+\right)$) for backward integration (control design) and knowledge of the system state at $t = t_k^-$ (i.e., $\boldsymbol{x}_k^-$) for forward integration (simulations), the terminal and initial time instants must be excluded from impulsive application times, that is: $t_k \in (t_0, t_\mathrm{f})$.

5 | ILLUSTRATIVE EXAMPLE

The functionality of the passivity-based control design frameworks proposed in Sections 3.4 and 3.5 is evaluated in this section through a multi-state mass-spring system shown in Figure 3. In this regard, the hybrid numerical algorithm described in Section 3.3 is first executed to compute the passivity-based control gains the utilization of which in the hybrid output dynamics of the plant satisfies the passivity specifications. Interconnecting the passive plant with an input strictly passive controller, which individually adopts compensators of static and dynamic forms, through negative feedback, the stability properties of the resultant closed-loop system are then assessed in Sections 5.1 and 5.2, respectively. Under the influence of continuous-time forces acting on masses 1 and 2 along with a single impulsive action on mass 2, the equations of motion for the mass-spring system can be formulated in a state-space representation as follows:

$$\dot{\boldsymbol{x}}(t) = \begin{bmatrix} x_3 \\ x_4 \\ \left(\kappa_2 x_2 - x_1\left(\kappa_1 + \kappa_2\right) - \kappa_2\alpha_2^2\left(x_1^3 - x_2^3\right) - \kappa_1\alpha_1^2 x_1^3\right)/m_1 \\ \left(\kappa_2\left(x_1 - x_2\right) + \kappa_2\alpha_2^2\left(x_1^3 - x_2^3\right)\right)/m_2 \end{bmatrix} + \begin{bmatrix} 0 & 0 \\ 0 & 0 \\ \cos(\omega t)/m_1 & 0 \\ 0 & \cos(\omega t)/m_2 \end{bmatrix} \boldsymbol{u}_{ct} + \sum_{k=1}^{\kappa} \begin{bmatrix} 0 \\ 0 \\ 0 \\ 1/m_2 \end{bmatrix} u_{ds,k}\delta\left(t - t_k\right),$$

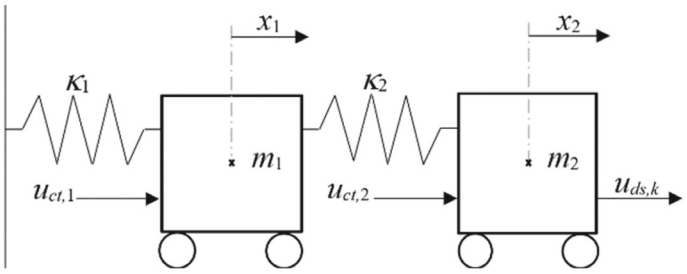

FIGURE 3 Schematic representation of mass-spring system under action of continuous-time and discrete-time forces.

where $\boldsymbol{x} = \begin{bmatrix} x_1 & x_2 & x_3 & x_4 \end{bmatrix}^{\mathrm{T}}$, $m_1 = 1\,\mathrm{kg}$, $m_2 = 0.5\,\mathrm{kg}$, $\alpha_1 = 1$, $\alpha_2 = 2$, $\kappa_1 = 1\,\mathrm{N/m}$, $\kappa_2 = 1.5\,\mathrm{N/m}$, $\omega = 1\,\mathrm{Hz}$, and $\delta(t)$ denotes the Dirac delta function located at each impulsive instant t_k.

With $\boldsymbol{f}_{ct}$, $\boldsymbol{g}_{ct}$, $\boldsymbol{f}_{ds}$, and $\boldsymbol{g}_{ds}$ coming directly from the hybrid equations of motion; stability region, $\boldsymbol{\Omega}$, basis functions, $\boldsymbol{\Phi}_N(\boldsymbol{x})$, impulsive application instants, the boundary conditions at the terminal time, $\boldsymbol{C}_{\mathrm{f}}$, and weighting functions, $\boldsymbol{l}_{ct}$ and $\boldsymbol{l}_{ds}$, remain to be determined. Since there are no kinematical limitations for the displacement and velocity components of both point masses, their domain of possible values is accordingly selected on the basis of practical considerations as follows:

$$\boldsymbol{\Omega} = \begin{bmatrix} -3 & 3 \end{bmatrix}_{x_1} \times \begin{bmatrix} -3 & 3 \end{bmatrix}_{x_2} \times \begin{bmatrix} -1 & 1 \end{bmatrix}_{x_3} \times \begin{bmatrix} -1 & 1 \end{bmatrix}_{x_4},$$

where the position and velocity quantities are expressed in m and m/s, respectively.

Basis functions are the next set of parameters to be appropriately determined. As is apparent, the dynamics of the system involve two nonlinear terms, namely x_1^3 and x_2^3. For the control to adequately capture these nonlinear terms, the quadratic basis elements obtained by the second-order expansion of the states must, thus, be augmented by additional higher-order terms. Since x_3 and x_4 act as the gain-effective states for the problem in hand, two basis elements in the form of $x_1^3 x_3$ and $x_2^3 x_3$ (or equivalently $x_1^3 x_4$ and $x_2^3 x_4$) are accordingly appended to the resultant set of quadratic basis elements to fulfill the characteristic requirements as follows: $\left\{x_1^2, x_1x_2, x_2^2, x_3^2, x_3x_4, x_4^2, x_1^3x_3, x_2^3x_3\right\}$.

By increasing the number of basis elements in a manner consistent with the characteristic requirements, the quantity requirement is ultimately met at $N = 14$, and the following set of basis functions are accordingly obtained:

$$\boldsymbol{\Phi}_N(\boldsymbol{x}) = \left\{x_1^2, x_1x_2, x_2^2, x_3^2, x_3x_4, x_4^2, x_1^3x_3, x_2^3x_3,\ x_1^4, x_1^2x_2^2, x_2^4, x_3^4, x_3^2x_4^2, x_4^4\right\}.$$

Assuming a prescribed set of impulsive application times, five equally spaced impulses, the applications of which result in satisfactory performance, are selected for this problem, that is, $\mathcal{K} = 5$.

The boundary conditions at the terminal time, $\boldsymbol{C}_{\mathrm{f}}$, play a crucial role in producing acceptable results. Owing to the time-varying nature of the passivity-based control gains $\boldsymbol{C}_N(t)$, blind selection of $\boldsymbol{C}_{\mathrm{f}}$ can lead to undesirable gains with unbounded growth in $\boldsymbol{C}_N(t)$ backward, thereby destroying the control design. The following boundary conditions at the terminal time are therefore selected to obtain satisfactory performance:

$$\boldsymbol{C}_{\mathrm{f}} = \left[0, 1, 1, 10^2, 10, 10^2, 1, 1, 0, 1, 1, 10^2, 10, 10^2\right]^{\mathrm{T}}.$$

Moreover, by considering $\boldsymbol{l}_{ct}$ and $\boldsymbol{l}_{ds}$ in the form of $\boldsymbol{l}_{ct}(\boldsymbol{x}, t) = \boldsymbol{\mathcal{L}}_{ct}\boldsymbol{x}$ and $\boldsymbol{l}_{ds}\left(\boldsymbol{x}_k^-, t_k^-\right) = \boldsymbol{\mathcal{L}}_{ds}\boldsymbol{x}_k^-$, where $\boldsymbol{\mathcal{L}}_{ct} \in \mathbb{R}^{p_{ct} \times n}$ and $\boldsymbol{\mathcal{L}}_{ds} \in \mathbb{R}^{p_{ds} \times n}$ are assumed to be constant, the following matrices are selected to weight the system state:

$$\boldsymbol{\Theta}_{ct} = \boldsymbol{\mathcal{L}}_{ct}^{\mathrm{T}}\boldsymbol{\mathcal{L}}_{ct} = diag\left(1 \quad 1 \quad 10^{-1} \quad 10^{-1}\right),$$

$$\boldsymbol{\Theta}_{ds} = \boldsymbol{\mathcal{L}}_{ds}^{\mathrm{T}}\boldsymbol{\mathcal{L}}_{ds} = diag\left(1 \quad 1 \quad 10^{-1} \quad 10^{-1}\right).$$

As is expected, a weighing matrix with larger diagonal terms results in performance whose transient response approaches the equilibrium faster.

5.1 | Stabilization via static compensator

In this section, the passivity-based control design framework equipped with a static constant-gain compensator is employed to stabilize the mass-spring system shown in Figure 3. To this end, the continuous-time and discrete-time positive proportional parameters used in the feedback loop to guarantee input strictly passivity are tuned to $\boldsymbol{K}_{ct} = \left(65 \times 10^{-2}\right) \mathbf{1}_{2\times 2}$ and $K_{ds} = 10^{-2}$, respectively. These parameters, in fact, serve to panelize the continuous-time and impulsive control effort.

The simulation results associated with the static compensator are shown in Figures 4 and 5 under the influence of the initial conditions $\boldsymbol{x}(0) = \begin{bmatrix} 10^{-1} & -2 \times 10^{-1} & 0 & 0 \end{bmatrix}^{\mathrm{T}}$ where the required computational time is 4.35 s. As is apparent, the time histories of the positions and velocities of point masses m_1 and m_2 demonstrate satisfactory performance in terms of transient response and steady-state behavior. By adjusting the size of the diagonal terms in the weighting matrices acting on the state and control, that is, $\boldsymbol{\Theta}_{ct}$ and $\boldsymbol{\Theta}_{ds}$ as against $\boldsymbol{K}_{ct}$ and K_{ds}, a trade-off between the speed of the response and control effort can be made to achieve satisfactory performance.

5.2 | Stabilization via dynamic compensator

In the next attempt, the passivity-based control architecture involving a dynamic compensator is used to stabilize the mass-spring system being considered. To this end, the following weighting matrices acing on the state and control in each

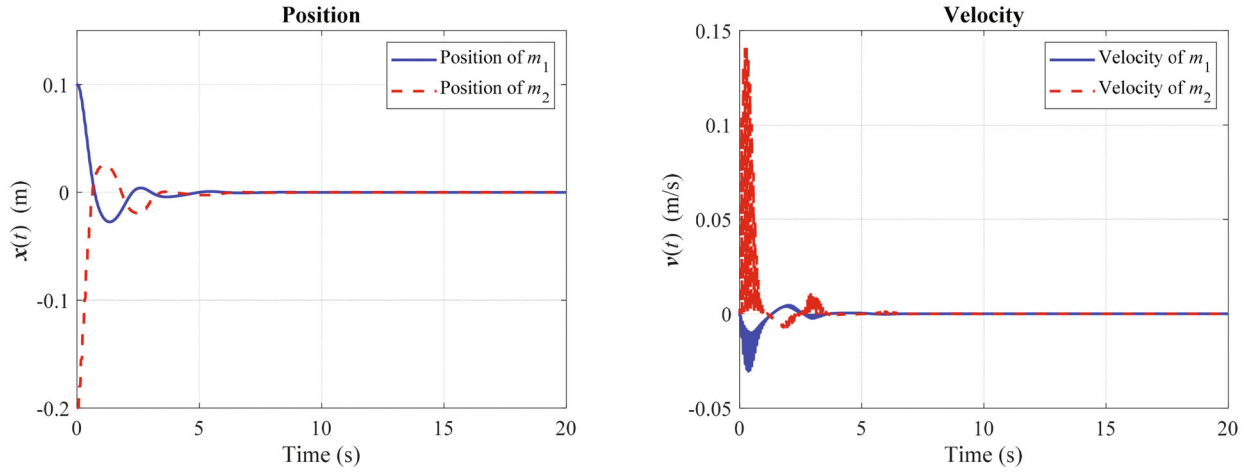

FIGURE 4 Time histories of position and velocity of mass-spring system with static compensator.

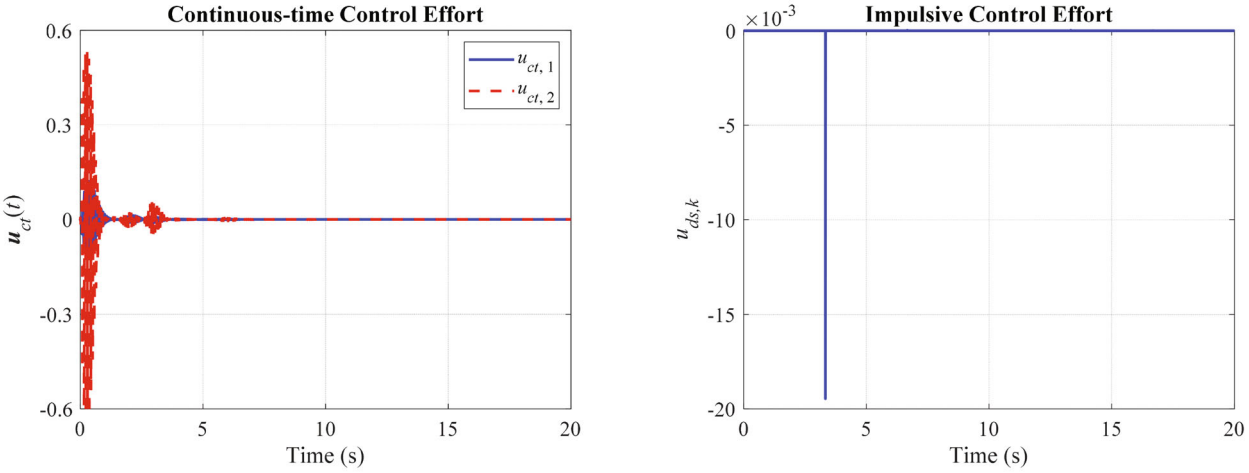

FIGURE 5 Time histories of continuous-time and discrete-time control inputs for mass-spring system under action of static compensator.

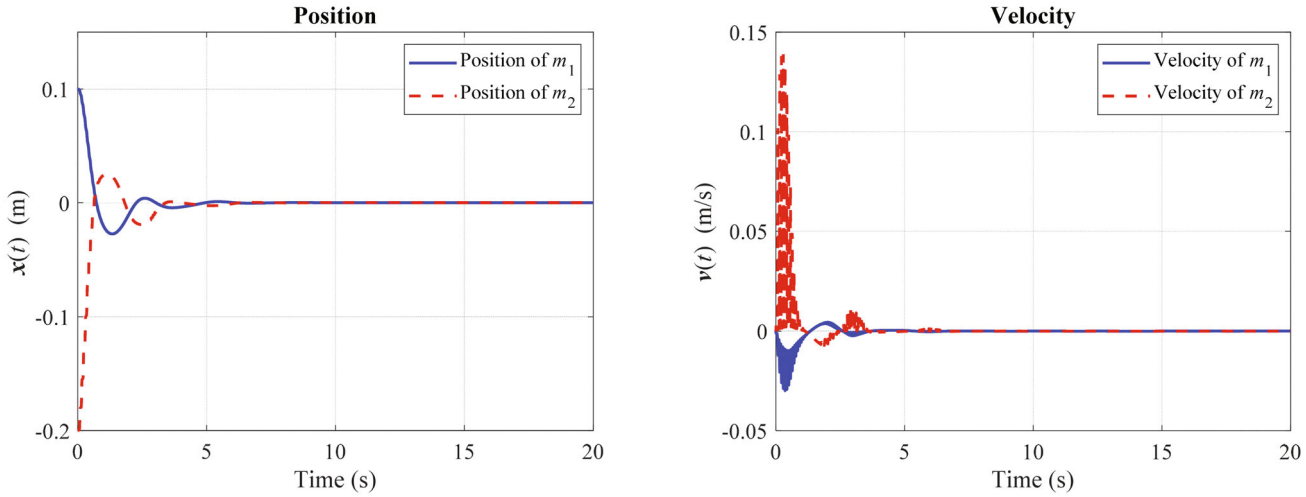

FIGURE 6 Time histories of position and velocity of mass-spring system with dynamic compensator.

continuous-time and discrete-time subsystem are first selected to tune the proposed hybrid LQR architecture formulated by (54) in preparation for rendering the dynamic compensator asymptotically stable:

$$\boldsymbol{Q}_{ct} = diag\begin{pmatrix} 5 & 5 & 5\times 10^{-1} & 5\times 10^{-1}\end{pmatrix}\ ,\ \boldsymbol{R}_{ct} = diag\begin{pmatrix} 10^{2} & 10^{2}\end{pmatrix},$$

$$\boldsymbol{Q}_{ds} = diag\begin{pmatrix} 10 & 10 & 10^{-1} & 10^{-1}\end{pmatrix}\ ,\ R_{ds} = 10^{7}.$$

Next, the following parameters are selected to simultaneously erect the interacting set of equations given by (59) to be integrated backward in time in order to compute $\boldsymbol{P}(t)$ to be used in (60), (62), and (63):

$$\boldsymbol{\Xi}_{ct} = \boldsymbol{L}_{ct}^{\mathrm{T}}\boldsymbol{L}_{ct} = diag\begin{pmatrix} 4\times 10^{-1} & 4\times 10^{-1} & 10 & 10\end{pmatrix},$$

$$\boldsymbol{\Xi}_{ds} = \boldsymbol{L}_{ds}^{\mathrm{T}}\boldsymbol{L}_{ds} = diag\begin{pmatrix} 6\times 10^{-1} & 6\times 10^{-1} & 10^{2} & 10^{2}\end{pmatrix},$$

$$\boldsymbol{P}_{\mathrm{f}} = \begin{bmatrix}\boldsymbol{P}_{\mathrm{f},1} & \boldsymbol{P}_{\mathrm{f},2}\\ \boldsymbol{P}_{\mathrm{f},2} & \boldsymbol{P}_{\mathrm{f},3}\end{bmatrix},$$

where $\boldsymbol{P}_{\mathrm{f},1} = \boldsymbol{0}_{2\times 2}$, $\boldsymbol{P}_{\mathrm{f},2} = \boldsymbol{1}_{2\times 2}$, and $\boldsymbol{P}_{\mathrm{f},3} = \boldsymbol{1}_{2\times 2}$. In this regard, $\boldsymbol{\Xi}_{ct}$ and $\boldsymbol{\Xi}_{ds}$ serve, respectively, to weight the continuous evolution of the state in the flow manifold and instantaneous changes in the state of the system in the jump manifold. Lastly, the continuous-time and discrete-time positive parameters used in (61) and (63), the utilization of which ensures input strict passivity via (30) and (33), are tuned to $\epsilon_{ct} = 65\times 10^{-2}$ and $\epsilon_{ds} = 10^{-5}$, respectively.

The simulation results associated with the dynamic compensator are depicted in Figures 6 and 7 under the exertion of the initial conditions $\boldsymbol{x}(0) = \begin{bmatrix}10^{-1} & -2\times 10^{-1} & 0 & 0\end{bmatrix}^{\mathrm{T}}$ where the required computational time is 7.39 s. As is evident, the hybrid passivity-based controller wields authority effectively to stabilize the states of the system with reasonably quick and well-damped responses for all position and velocity components. By increasing ϵ_{ct}, ϵ_{ds}, $\boldsymbol{Q}_{ct}$, and $\boldsymbol{Q}_{ds}$ (while $\boldsymbol{R}_{ct}$ and $\boldsymbol{R}_{ds}$ are decreased or remain constant), the proposed control scheme drives position and velocity components to zero faster. This improved performance occurs, however, at the expense of larger continuous-time and impulsive control effort, which is practically undesirable. Furthermore, the superior performance of the dynamic compensator can be observed in comparison to the static compensator by quantitatively assessing their functionalities via defining and computing root-mean-square norms in terms of the state and control inputs over the entire operating time.

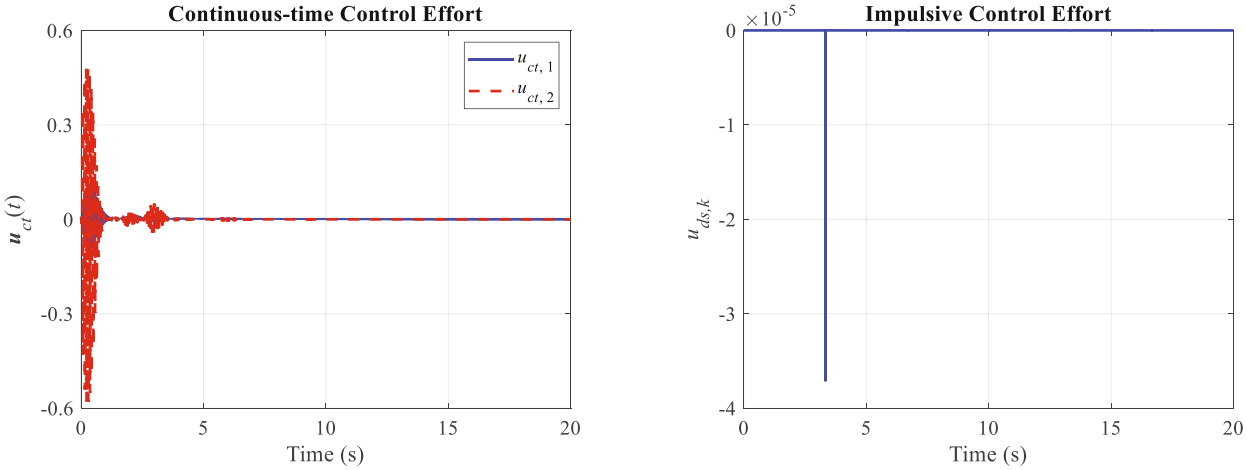

FIGURE 7 Time histories of continuous-time and discrete-time control inputs for mass-spring system under action of dynamic compensator.

6 | CONCLUSION

Two passivity-based control architectures for hybrid nonlinear dynamical systems involving an interacting mixture of continuous-time and discrete-time dynamics whose dynamical properties evolve periodically over time have been developed in this article. By deriving the KYP conditions characterizing dissipativity for hybrid nonlinear time-dependent dynamical systems, a hybrid numerical framework was then proposed to solve the resultant equations in an interacting manner. Utilizing the aforementioned KYP conditions and the passivity theorem simultaneously, compensators of static and dynamic structures were then developed to establish stable closed-loop dynamics. To summarize, the proposed hybrid control schemes enjoy several advantages: (1) the approximate control laws are in an explicit form of output feedback; (2) the control laws remain stable when the approximation is truncated at a finite degree of complexity; (3) the stability region is specified by the user; (4) computations are performed off-line; (5) the system performance is anticipated to exhibit enhanced robustness with respect to uncertainties and measurement noise effects; and (6) the resultant control laws, the synthesis of which is based upon the full nonlinear dynamics of the system, can be exploited over the entire operating range of the system.

CONFLICT OF INTEREST STATEMENT

There is no conflict of interest to declare.

DATA AVAILABILITY STATEMENT

Data sharing is not applicable to this article as no datasets were generated or analyzed during the current study.

ORCID

Esmaeil Sharifi https://orcid.org/0000-0003-2244-8773

REFERENCES

1. Haddad WM, Chellaboina V, Nersesov SG. *Impulsive and Hybrid Dynamical Systems*. Princeton University Press; 2006.
2. van der Schaft AJ, Schumacher H. *An Introduction to Hybrid Dynamical Systems*. Springer; 2000.
3. Forbes JR, Damaren CJ. Linear time-varying passivity-based attitude control employing magnetic and mechanical actuation. *J Guid Control Dyn*. 2011;34(5):1363-1372.
4. Tomlin C, Pappas GJ, Sastry S. Conflict resolution for air traffic management: a study in multiagent hybrid systems. *IEEE Trans Autom Control*. 1998;43(4):509-521.
5. Žefran M, Bullo F, Stein M. A notion of passivity for hybrid systems. *40th IEEE Conference on Decision and Control*. Piscataway; 2001.
6. Goebel R, Sanfelice RG, Teel AR. *Hybrid Dynamical Systems: Modeling, Stability, and Robustness*. Princeton University Press; 2012.
7. Forbes JR, Damaren CJ. Single-link flexible manipulator control accommodating passivity violations: theory and experiments. *IEEE Trans Control Syst Technol*. 2012;20(3):652-662.

8. Lang X, Damaren CJ, Cao X. Hybrid finite-frequency attitude control motivated by Volterra series. *J Guid, Control Dyn*. 2020;43(8):1432-1443.
9. Desoer CA, Vidyasagar M. Linear Systems. *Feedback Systems: Input–Output Properties*. Academic Press; 1975.
10. Popov VM. Absolute stability of nonlinear Systems of Automatic Control. *Autom Remote Control*. 1961;22(8):961-979.
11. Yakubovich VA. The solution of certain matrix inequalities in automatic control theory. *Soviet Math*. 1962;3(2):620-623.
12. Kalman RE. Lyapunov functions for the problem of Lur'e in automatic control. *Nat Acad SciUSA*. 1963;49(2):201-205.
13. Anderson BDO. A system theory criterion for positive real matrices. *SIAM J Control*. 1967;5(2):171-182.
14. Willems JC. Dissipative dynamical systems, part I: general theory. *Arch Ration Mech Anal*. 1972;45(5):321-351.
15. Willems JC. Dissipative dynamical systems, part II: linear systems with quadratic supply rates. *Arch Ration MechAnal*. 1972;45(5):352-393.
16. Moylan PJ. Implications of passivity in a class of nonlinear systems. *IEEE Trans Autom Control*. 1974;19(4):373-381.
17. Hill D, Moylan PJ. The stability of nonlinear dissipative systems. *IEEE Trans Autom Control*. 1976;21(5):708-711.
18. Hill DJ, Moylan PJ. Stability results for nonlinear feedback systems. *Automatica*. 1977;13(4):377-382.
19. Haddad WM, Chellaboina V, Kablar NA. Nonlinear impulsive dynamical systems. Part I: stability and Dissipativity. *Int J Control*. 2001;74(17):1631-1658.
20. Haddad WM, Chellaboina V, Kablar NA. Nonlinear impulsive dynamical systems. Part II: stability of feedback interconnections and optimality. *Int J Control*. 2001;74(17):1659-1677.
21. Moreno JA. Approximate observer error linearization by dissipativity methods. *Control and Observer Design for Nonlinear Finite and Infinite Dimensional Systems*. Springer Berlin Heidelberg; 2005:35-51.
22. Avilés JD, Moreno JA. Dissipative observers for discrete-time nonlinear systems. *J Franklin Inst*. 2018;355(13):5759-5770.
23. Avilés JD, Moreno JA. Dissipative interval observer Design for Discrete-time Nonlinear Systems. *Asian J Control*. 2020;22(4): 1422-1436.
24. W. M. Haddad, . V. Chellaboina and E. August, Stability and Dissipativity theory for discrete-time nonnegative and compartmental dynamical systems, *Int J Control,* vol. 76, pp. 1845–1861, 2003.
25. Haddad WM, Chellaboina V, Rajpurohit T. Dissipativity theory for nonnegative and compartmental dynamical systems with time delay. *IEEE Trans Autom Control*. 2004;49:747-751.
26. Haddad WM, Chellaboina V, Hui Q, Nersesov SG. Vector Dissipativity theory for large-scale impulsive hybrid dynamical systems. *Math Probl Eng*. 2004;2004(3):225-262.
27. Haddad WM, Chellaboina V, Nersesov SG. Vector Dissipativity theory and stability of feedback interconnections for large-scale nonlinear dynamical systems. *Int J Control*. 2004;77:907-919.
28. Haddad WM, Nersesov SG, Chellaboina V. Energy-based control for hybrid port-controlled Hamiltonian systems. *Automatica*. 2003;39:1425-1435.
29. W. M. Haddad, T. Rajpurohit and . X. Jin, Energy-based feedback control for stochastic port-controlled Hamiltonian systems, *Automatica,* vol. 97, pp. 134–142, 2018.
30. Rajpurohit T, Haddad WM. Dissipativity theory for nonlinear stochastic dynamical systems. *IEEE Trans Autom Control*. 2017;62(4):1684-1699.
31. Haddad WM, Jin X. Implications of Dissipativity, inverse optimal control, and stability margins for nonlinear stochastic regulators. *Int J Robust Nonlinear Control*. 2019;29:5499-5519.
32. Vatankhahghadim B, Damaren CJ. Magnetic attitude control with impulsive thrusting using the hybrid passivity theorem. *J Guid Control Dyn*. 2017;40(8):1860-1876.
33. Fletcher CAJ. *Computational Galerkin Methods*. Springer; 1984.
34. Quarteroni A, Sacco R, Saleri F. *Numerical Mathematics*. Springer; 2000.
35. Benhabib RJ, Iwens RP, Jackson RL. Stability of large space structure control systems using positivity concepts. *J Guid Control Dyn*. 1981;4(5):487-494.
36. Sobiesiak LA, Damaren CJ. Optimal continuous/impulsive control for Lorentz-augmented spacecraft formations. *J Guid Control Dyn*. 2015;38(1):151-157.
37. Beard R, Saridis G, Wen J. Galerkin approximations of the generalized Hamilton-Jacobi-bellman equation. *Automatica*. 1997;33(12):2159-2177.
38. Beard R, McLain T. Successive Galerkin approximation algorithms for nonlinear optimal and robust control. *Int J Control*. 1998;71(5):717-743.
39. Boyce WE, DiPrima RC. *Elementary Differential Equations and Boundary Value Problems*. John Wiley & Sons; 1992.

How to cite this article: Sharifi E, Damaren CJ. Passivity-based control design frameworks for hybrid nonlinear time-varying dynamical systems. *Int J Robust Nonlinear Control*. 2023;1-21. doi: 10.1002/rnc.6818